NATIONAL RADIO ASTRONOMY OBSERVATORY
SOCORRO, NEW MEXICO
VERY LARGE ARRAY PROGRAM

VLA ELECTRONICS MEMORANDUM NO. 177

SPURIOUS RESPONSES IN THE VLA CIRCULAR WAVEGUIDE SYSTEM.

J. Archer

August 1978

1.0 INTRODUCTION

The Very Large Array is a high sensitivity, multi-frequency aperture synthesis radio telescope, which will provide high resolution brightness maps of cosmic radio sources (Heeschen [1977]). The array is currently being constructed in central New Mexico by the National Radio Astronomy Observatory under contract from the National Science Foundation. The VLA consists of 27 antennas arranged along the arms of a Y configuration. Each arm is between 19 and 21 kilometers in length and may be comprised of up to nine operational antennas at a given time, located at any of 24 observing stations. A low-loss, wideband transmission system is required for communication between any antenna and the central Control Building. The design of the millimeter wavelength waveguide system adopted for the VLA has been described by Weinreb, Predmore, Ogai and Parrish [1977].

A single 60 mm diameter helix lined waveguide carrying the low-loss TE_{01} mode and extending along each arm of the Y is sufficient to communicate all signals to and from the nine antennas on an arm.

In order to avoid a large number of cables and the necessity for having electronic equipment at more than one location at each antenna, 20 mm diameter helix lined waveguide carries the signals from a directional coupler in the 60 mm trunk waveguide to the vertex equipment room of each antenna. An antenna is assigned a 1 GHz bandwidth communication channel and eleven channels (2 spare) are allocated in the 27 to 53 GHz range. Within these 1 GHz single sideband modulated channels, the the signals communicated from the control building to each antenna are:

(1) a pair of local oscillator reference tones separated in frequency by 600 MHz. The lower frequency tone carries a 5 MHz amplitude modulation used as a phase ambiguity resolver. The difference signal between the tones provides a 600 MHz phase stable reference signal for each antenna local oscillator system. The relative phase of the difference signal at each antenna is determined as a function of the electrical length of the waveguide by a system which measures the phase difference between the outgoing 600 MHz reference and signals returned from each antenna by the LO system encoded as a similar pair of reference tones,

(2) digital command signals for antenna and receiver electronics control, which are amplitude modulated onto the higher frequency reference tone.

The return signals to the control building from each antenna are similar in nature to (1) and (2) above, but with the addition of four 50 MHz wide analogue IF signals in the frequency range 1.3 to 1.7 GHz USB relative to the carrier. The transmission system

amplitude response is required to be flat to within ± 1 dB over this 50 MHz bandwidth. The forward and return signals are time multiplexed with a transmission cycle, 1 msec outward, 52 msec return.

Small scale frequency dependent variations in the phase and amplitude response of the waveguide system can significantly affect the performance of the antenna array, especially when the frequency dependence varies with time. Local oscillator phase relationships at the antennas can be modified and the phase and amplitude relationships between IF passbands can be altered, when the variations occur within small frequency intervals. For these reasons the maximum variation in the mean power transmission response of the waveguide network between any antenna and the control building (the maximum mean square variation in the TE_{01} mode amplitude response) has been specified to be 0.05 dB in any 10 MHz band. (See Appendix C)

In this paper the effect of the most prominent sources of transmission ripples in the waveguide system on array performance is investigated. Methods for determining the dominant sources of higher order mode interaction are described and practical methods for the reduction of the significance of spurious mode coupling are discussed.

2.0 REFLECTIONS AND SPURIOUS MODES IN A WAVEGUIDE NETWORK

Frequency dependent phase and amplitude variations in the waveguide system transfer function may be attributed to two broadly classified mechanisms: (1) mode conversion-reconversion between the TE_{01} mode

and unwanted modes at separated points in the waveguide network,

(2) TE_{01} mode reflections between separated discontinuities.

In helix waveguide, the significant higher order modes are all TE_{on} modes. For two mode conversion-reconversion sources in the transmission system separated by a distance ℓ, with mode conversion coefficients C_1, C_2, the TE_{01} mode amplitude transmission function is:

$$T_{01} = 1 + C_1 C_2 e^{-\Delta\alpha\ell} e^{-j\Delta\beta\ell} \tag{2.1}$$

where $\Delta\alpha$ is the difference in attenuation constant between the unwanted and TE_{01} modes ($\alpha_{on}-\alpha_{01}$) (about 2 dB for TE_{02} and TE_{01} modes). $\Delta\beta$ is similarly, the difference in propagation constants ($\beta_{on}-\beta_{01}$). The perturbation causes a deviation, $\Delta\phi$, in the phase of the difference signal between two tones f, f' ($\frac{f'}{f}\sim 1$) transmitted along the waveguide section given by (Ogai [1977])

$$\Delta\phi = 2C_1 C_2 e^{-\Delta\alpha\ell} \cos\left[\frac{(\Delta\beta+\Delta\beta')}{2}\ell\right]\left[\sin\frac{(f-f')}{f_r}\pi\right] \tag{2.2}$$

where $\Delta\beta$,$\Delta\beta$ are the differences in propagation constant at frequencies f and f' respectively

and f_r, the scale size of the spurious mode frequency dependence of the transfer function is given by

$$f_r = \frac{2\pi}{\ell \cdot \frac{d}{df}(\Delta\beta)}$$

When two TE_{01} mode reflection sources interact over a distance ℓ, with reflection coefficients ρ_1, ρ_2, the TE_{01} mode transmission function is:

$$T_{01} = 1 + \rho_1 \rho_2 e^{-2\alpha_{01}\ell} e^{-2j\beta_{01}\ell}. \tag{2.3}$$

The resulting pilot signal phase deviation is given by (Ogai [1977])

$$\Delta\phi = 2\rho_1\rho_2 \, e^{-2\alpha_{01}\ell} \cos\left[(\beta_{01}+\beta_{01}')\ell\right] \sin\left[\frac{(f-f')}{f_r} \cdot \pi\right] \tag{2.4}$$

where $f_r = \dfrac{\pi}{\ell \cdot \dfrac{d}{df}(\beta_{01})}$ represents the scale of the reflection dependence of the transfer function.

3.0 THE CASE OF MANY NON-UNIFORMITIES IN A WAVEGUIDE LINE

A complete analysis of the performance of the VLA waveguide system requires a consideration of the interaction between many mode conversion and single mode reflection sources in the network. Furthermore, an understanding of the behavior of the various components which give rise to performance degradation is essential. The general theory for multi-component interaction has been developed extensively elsewhere (e.g., Rowe and Warters [1962]). In the present paper the theory is modified for the special case of the VLA. The VLA network is significantly different from other circular TE_{01} mode waveguide applications in that each trunk waveguide arm has many directional couplers installed

at irregular intervals. The sector couplers (Archer et al [1978]), can give rise to single mode reflections and spurious mode conversion-reconversion in the main 60 mm diameter waveguide. Furthermore, mode conversion-reconversion in the coupled line can occur, since the device is intrinsically a broadband power divider for all circular TE_{0n} modes. The resultant interactions between non-uniformities in the exposed antenna waveguide can give rise to frequency dependent features in the system transfer function which have a significant dependence on ambient air temperatures.

3.1 Mode Conversion-Reconversion Effects

Consider the model waveguide system indicated in Figure 1. The main line transmission matrix, s_k, for the kth mode conversion source is

$$s_k = \begin{bmatrix} \sqrt{1-C_k^2} & C_k \\ C_k & \sqrt{1-C_k^2} \end{bmatrix} \tag{3.1}$$

where C_k is the symmetrical ($TE_{01} \leftrightarrow TE_{on}$) coupling coefficient. The transmission matrix for the kth mode conversion source and the subsequent length of ideal waveguide ℓ_k is

$$m_k = \begin{bmatrix} e^{-\Gamma_{01}\ell_k} & 0 \\ 0 & e^{-\Gamma_{0n}\ell_k} \end{bmatrix} \cdot s_k \tag{3.2}$$

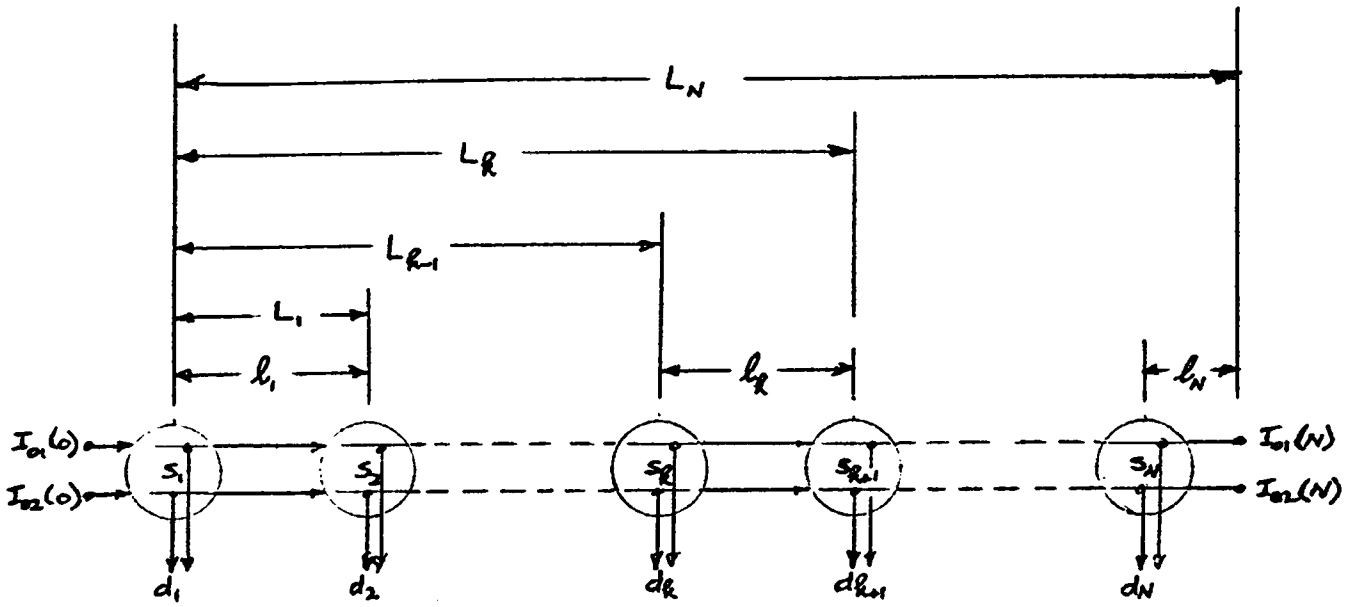

Figure 1

Discrete directional coupler/mode converters in ideal waveguide line

where Γ_{oi} is the propagation constant for the circular TE_{oi} mode. The total transmission matrix to the Nth coupler is

$$T = \prod_{k=N}^{1} m_k = \begin{bmatrix} t_{11} & t_{12} \\ t_{21} & t_{22} \end{bmatrix} \tag{3.3}$$

where the coupler losses have been neglected.

To second order in C_k, the TE_{01} mode amplitude response is given by, (Rowe & Warters [1962])

$$t_{11} \sim e^{-\Gamma_{01}L_N}\left[(1-\tfrac{1}{2}\sum_{i=1}^{N} C_i^2) + \sum_{i=1}^{N-1}\sum_{j=i+1}^{N} C_iC_j\, e^{\Delta\Gamma(L_{j-1}-L_{i-1})}\right] \tag{3.4}$$

where $L_k = \sum_{j=1}^{k} \ell_j$

and $\Delta\Gamma = \Gamma_{01} - \Gamma_{02}$.

Again, to second order in C_k, the TE_{02} mode amplitude at the input to Nth coupler is (Rowe and Warters [1962])

$$t_{21} \sim e^{-\Gamma_{02}L_N} \sum_{i=1}^{N-1} C_i e^{-\Delta\Gamma L_{i-1}}. \tag{3.5}$$

The Nth coupler in the transmission system converts some of the incident TE_{02} mode signal into TE_{01} mode in the coupled arm. Accordingly, if the coupled arm mode coupling coefficient is d_N, the effective normalized TE_{01} mode amplitude response at the coupled output of the Nth coupler is

$$t_{11}^{1} \sim e^{-\Gamma_{01}L_N}\left[1 - \sum_{i=1}^{N} C_i^2 + \sum_{i=1}^{N-1}\sum_{j=i+1}^{N} C_iC_j\, e^{\Delta\Gamma(L_{j-1}-L_{i-1})} + d_N \sum_{i=1}^{N-1} C_i\, e^{\Delta\Gamma(L_N-L_{i-1})}\right] = 1-\rho \tag{3.6}$$

The third and fourth terms in equation (3.6) result in a dependence of the TE_{01} amplitude response on transmission frequency.

Writing,

$$t_{11}^{1} = e^{-\Gamma_{01}L_N}(e^{-A}e^{j\theta})$$

if $\rho<<1$, the mean square variation in the attenuation constant, proportional to the mean variation in received power with frequency, is given by

$$\overline{\langle\delta A^2\rangle} \sim \tfrac{1}{2}\sum_{i=1}^{N-1}\sum_{j=i+1}^{N}\left[\varepsilon_i\varepsilon_j e^{\Delta\alpha(L_{j-1}-L_{i-1})}\right]^2 + \tfrac{1}{2}\delta_N\sum_{i=1}^{N-1}\left[\varepsilon_i e^{\Delta\alpha(L_N-L_{i-1})}\right]^2 \qquad (3.7)$$

where $\varepsilon_k = |C_k|$; $\delta_k = |d_k|$.

3.2 TE_{01} Mode Reflection Effects

A similar approach, using matrix methods applied to the configuration in Figure 2, yields the following expressions for the mean square variation in the TE_{01}, mode attenuation constant at the kth coupler for TE_{01} mode reflective interactions alone, (k>1)

$$\overline{\langle\delta A^2\rangle} \sim \tfrac{1}{2}\left\{\sum_{i=1}^{N}\left[|\rho_s\rho_{ci}|e^{-2\alpha_{01}L_i}\right]^2 + \sum_{j=1}^{k-1}\sum_{i=j+1}^{N}\left[|\rho_{ci}\rho_{cj}|e^{-2\alpha_{01}(L_i-L_j)}\right]^2 + \sum_{j=k+1}^{N}\left[|D_k\rho_{cj}|e^{-2\alpha_{01}(L_j-L_k)}\right]^2\right\} \qquad (3.8)$$

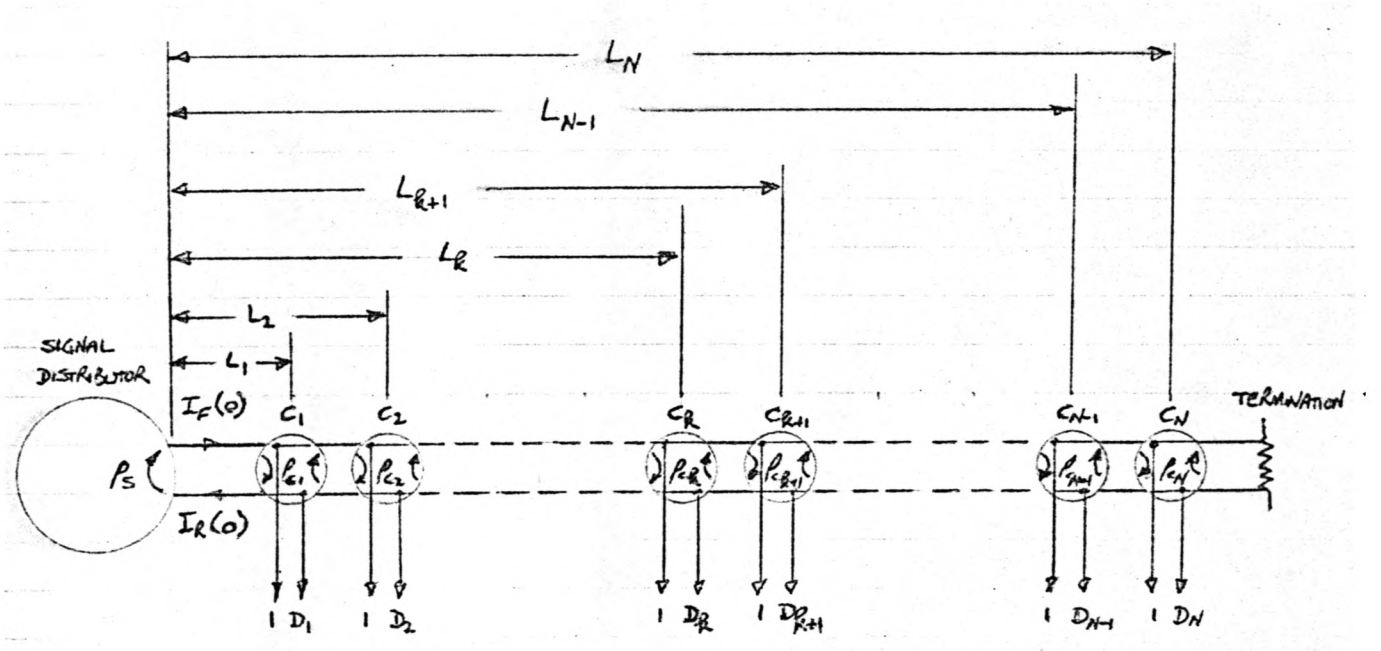

Figure 2

Discrete directional coupler/reflection sources in an ideal waveguide line.

where ρ_{ci} is the forward or reverse reflection coefficient (assumed identical) for the ith coupler,

ρ_s is the distribution box reflection coefficient,

D_i is the directivity of the ith coupler,

N is the total number of couplers on a given arm of the array.

The couplers were assumed lossless in the derivation of this expression.

4.0 WAVEGUIDE SYSTEM COMPONENTS

4.1 TE_{01} Mode Reflection and Transmission Properties

In order to understand the performance of the VLA waveguide communications network, it is necessary to determine the essential electrical characteristics of the constituent components and to identify those devices which have a significant effect on the overall transmission response. The TE_{01} mode reflection and transmission performance of the couplers, main trunk waveguide, antenna waveguide, modems and waveguide windows, tapers and distribution box have been determined by well-known standard techniques. The essential characteristics are summarized in Table 1.

4.2 Mode Conversion Properties

Attention is now turned to the mode conversion characteristics of the devices in the waveguide network. Special techniques

Device	Typical TE_{01} Mode Return Loss (27-50 GHz)	Typical TE_{01} Mode Insertion Loss (27-50 GHz)
Sector Couplers (9^{o} Sector)		
a) Main waveguide forward direction	-44 dB	-0.16 dB
b) Main waveguide reverse direction	-46 dB	-0.12 dB
c) Coupling from main waveguide	--	-23 dB
d) Reflection in coupled arm	-18 dB	--
e) Directivity	--	-12 dB
60 mm Waveguide Line	--	-1.3 dB/km
Beam Splitter Couplers (-10 dB Coupling)		
a) Main waveguide forward direction	-45 dB	-0.7 dB
b) Main waveguide reverse direction	-45 dB	-0.25 dB
c) Reflection in coupled arm	-45 dB	--
d) Directivity	--	-35 dB
Total Antenna Waveguide Loss	--	-4.0 dB
20 mm ϕ to 60 mm ϕ Tapers	-45 dB	-0.05 dB
Distribution Box (Circular w/g Port)	-20 dB	-5.0 dB ($TE^{\square}_{10}$ to TE^{o}_{01})
Modem/Waveguide Window at Design Frequency	-26 dB	--

Table 1

Reflection and Transmission Properties of Devices
Used in the VLA Waveguide System

have been developed to aid in the measurement of spurious mode coupling in the various circular waveguide components. As randomized segment length, helix-lined waveguide is used throughout the VLA system, non-circular TE_{mn}, TM_{mn} mode generation should not cause significant problems. Neither should circular electric mode generation due to waveguide coupling misalignments. The most significant sources of spurious circular electric mode conversion-reconversion would be expected to be the directional couplers, tapers and distribution box. Furthermore, interaction between the TE_{01} and TE_{02} modes would be expected to be the predominant source of perturbation to the transmission response of the waveguide system. The level of mode coupling in a given device can be determined by measuring the amplitude of the ripple introduced on the TE_{01} mode amplitude response when the device and a standard mode generator with known characteristics are placed at an appropriate separation in the waveguide line.

4.3 Design of a Standard Mode Coupler

To achieve high coupled mode purity it is most convenient to fabricate the TE_{02} standard mode generator to operate in 20 mm diameter waveguide. The concept of the device is indicated in Figure 3. It comprises a concentric dual step discontinuity in the circular waveguide with the diameter and step separation chosen to give the desired coupling and uniform coupling frequency response. The performance of the mode generator has been analyzed in the manner described in Appendix A. The

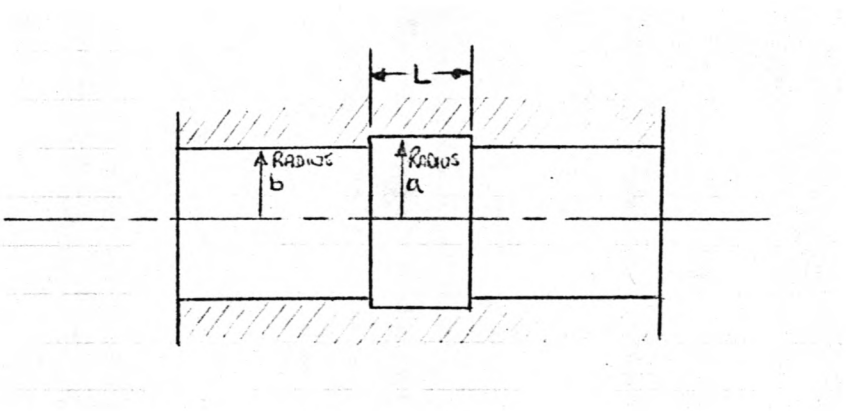

Figure 3

TE_{02} Mode Coupler for 20 mm Diameter Waveguide

systems of simultaneous equations in the Appendix have been solved numerically for the case where N, the number of modes considered in the solution, equals 10. This is sufficient to give the solution to better than 1% accuracy (Wexler [1967]). The inversion routine successively applies Gauss-pivotal techniques to the complex-valued system matrices defined by equations (A1.1) and (A1.3). The predicted TE_{02} mode coupling, TE_{01} mode insertion loss and return loss as functions of frequency are indicated in Figures 4, 5 and 6 for a range of mode generator dimensions.

Figure 4

Predicted and measured $TE_{01} \rightarrow TE_{02}$ mode coupling for two typical mode couplers

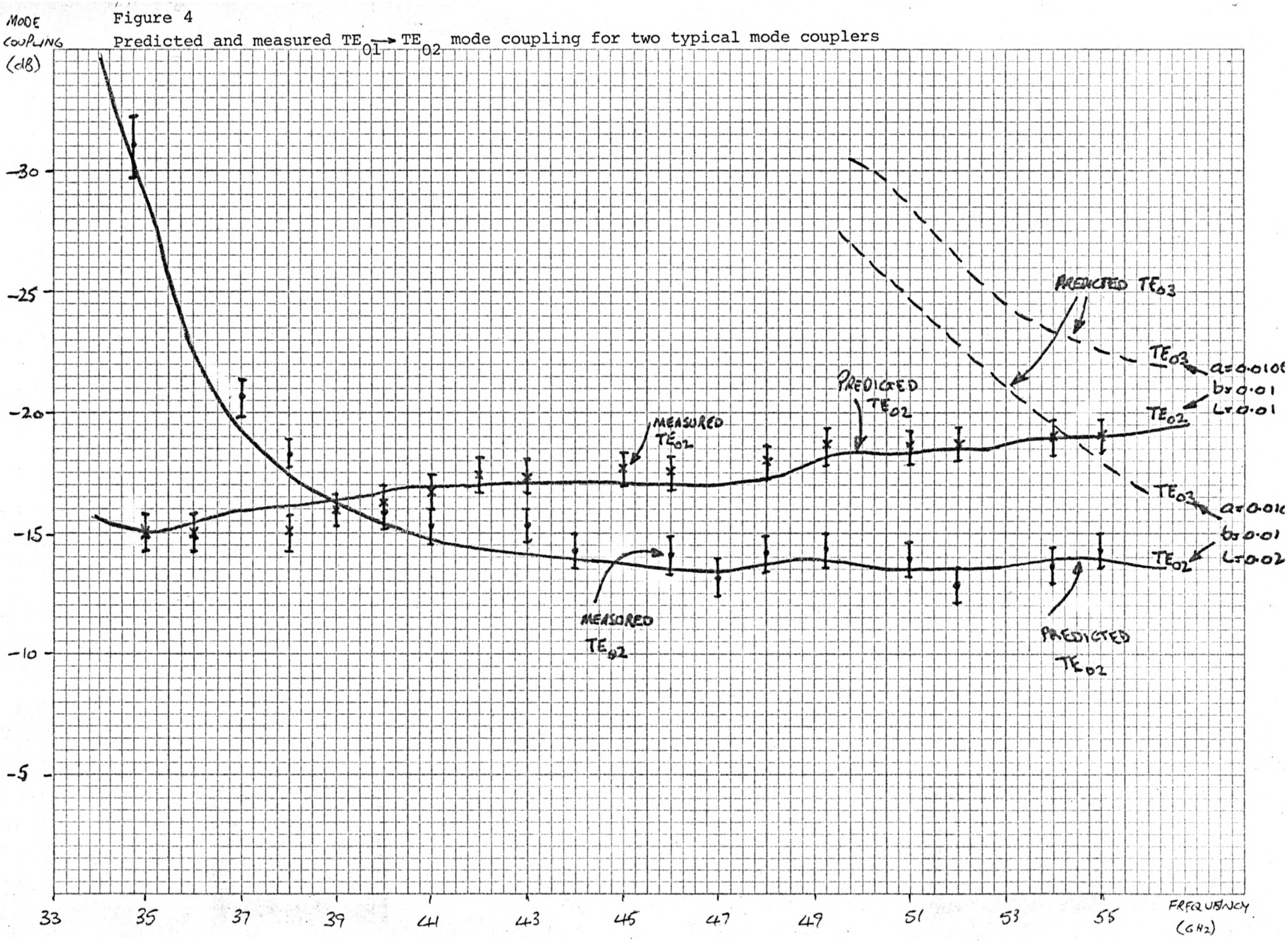

Figure 5

Predicted and measured insertion loss of two typical mode couplers (TE_{01} mode)

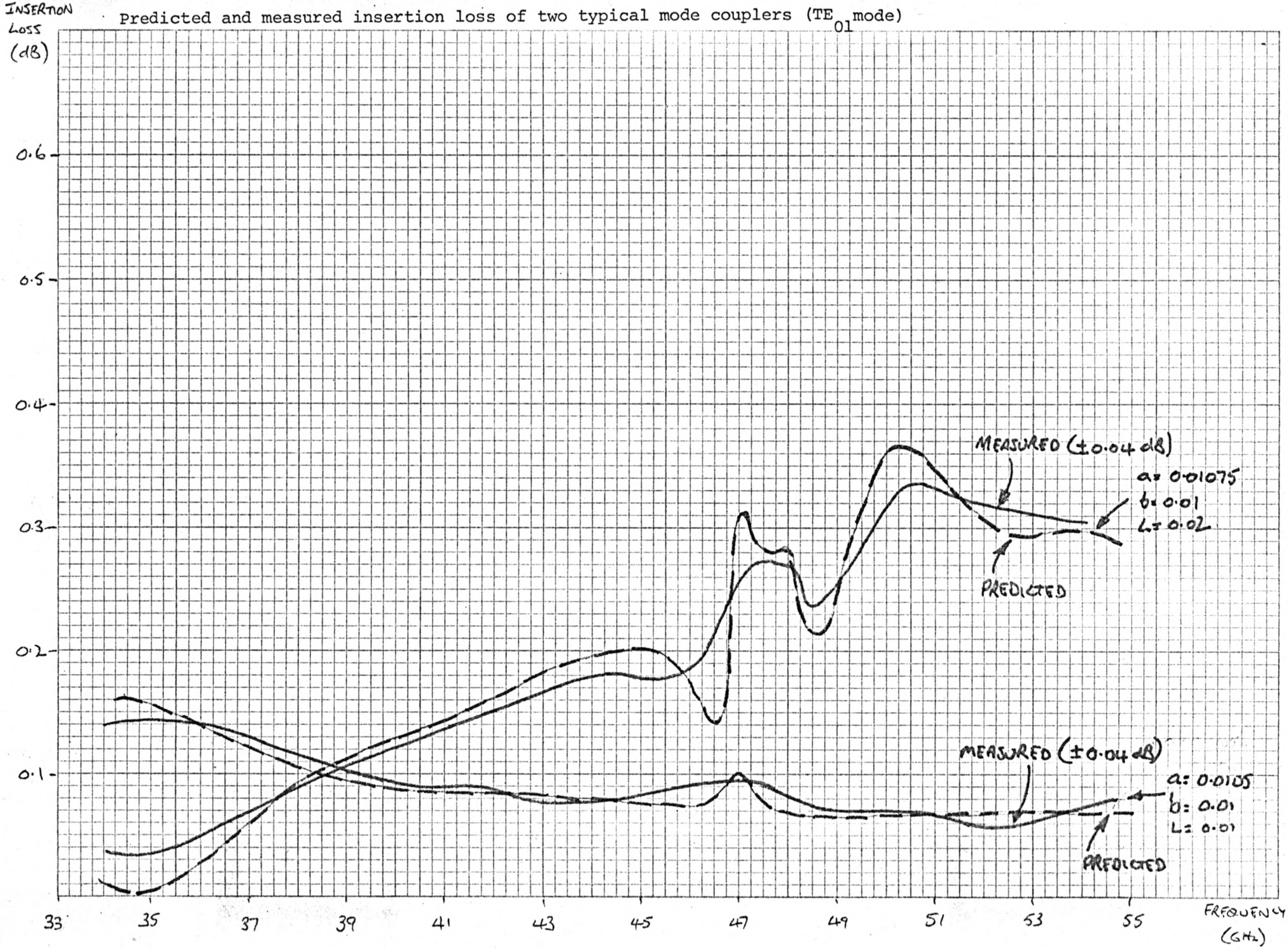

Figure 6

Predicted and measured return loss of two typical mode couplers

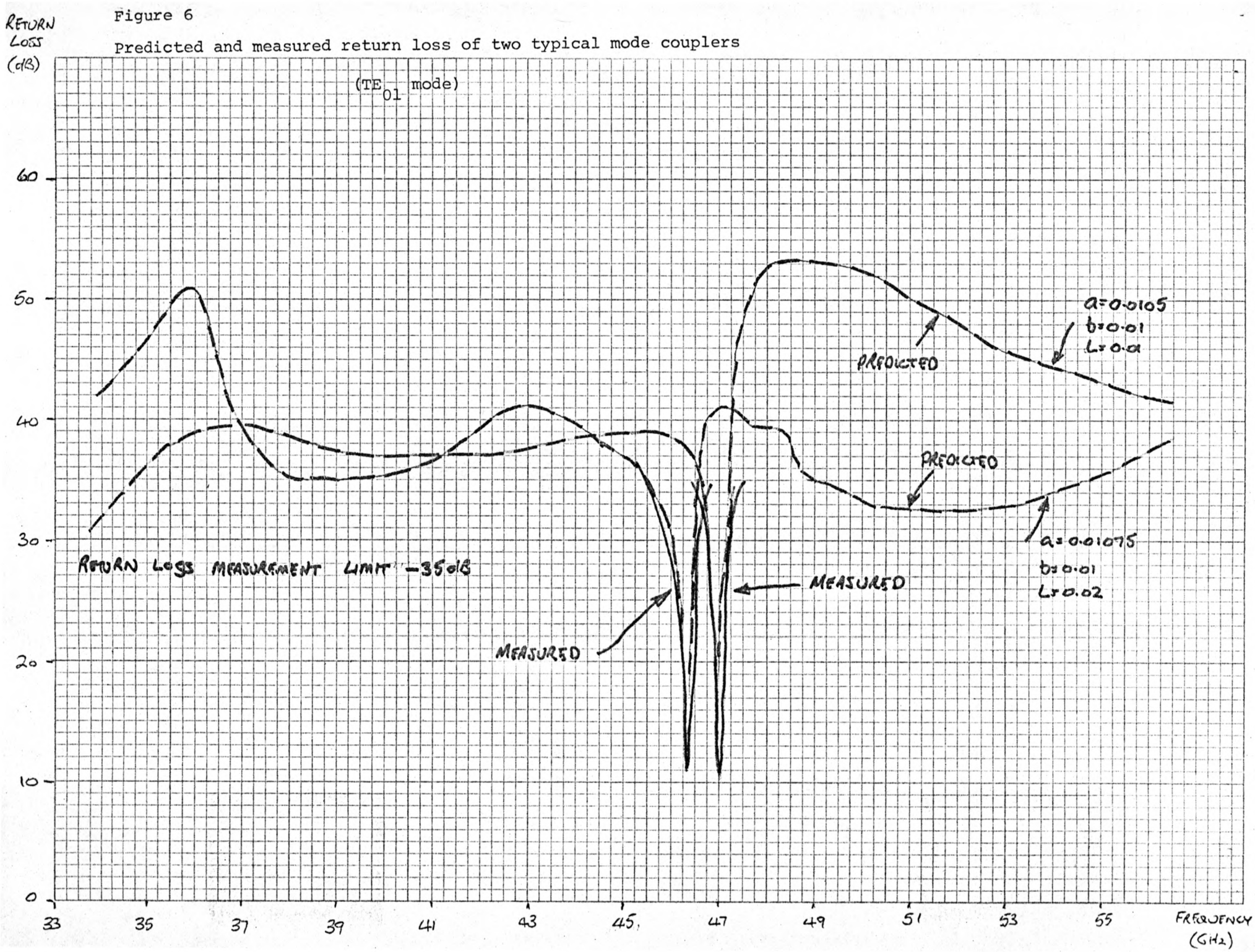

Mode generators of the above dimensions have been fabricated and their behavior experimentally evaluated by measuring the TE_{01} insertion loss and return loss as a function of frequency. The TE_{02} mode generation characteristics were determined by measuring the amplitude of the TE_{01} mode insertion loss ripple caused by two identical devices installed in a 20 mm waveguide line at a fixed separation. The experimental results are indicated in Figures 4, 5 and 6. As can be seen, good agreement is obtained between the theoretically predicted and the measured behavior.

4.4 Mode Conversion Characteristics of the Waveguide Components

Having determined the TE_{02} mode coupling of a given mode generator the device can be used as a standard in order to determine the TE_{02} mode coupling of any other device inserted in the 20 mm waveguide. The method is similar to that used for calibration of the generators. The mode coupler and the device under test are connected at opposite ends of a fixed length of waveguide and the TE_{02} mode coupling of the test unit inferred from the amplitude of the ripple impressed on the TE_{01} mode transmission response. Using this technique, the mode conversion versus frequency characteristics of a typical VLA distribution box (Figure 7) and a coupler main-waveguide to coupled arm response (Figure 8) have been determined. The step in the distribution box response near 40 GHz is due to the increased TE_{02} mode attenuation between the 20 mm diameter input port and the high band section (41.8 - 52.4 GHz) of the unit, which is connected via 5 meters of flexible 20 mm waveguide.

Figure 7

Distribution box TE_{02} mode generation characteristics

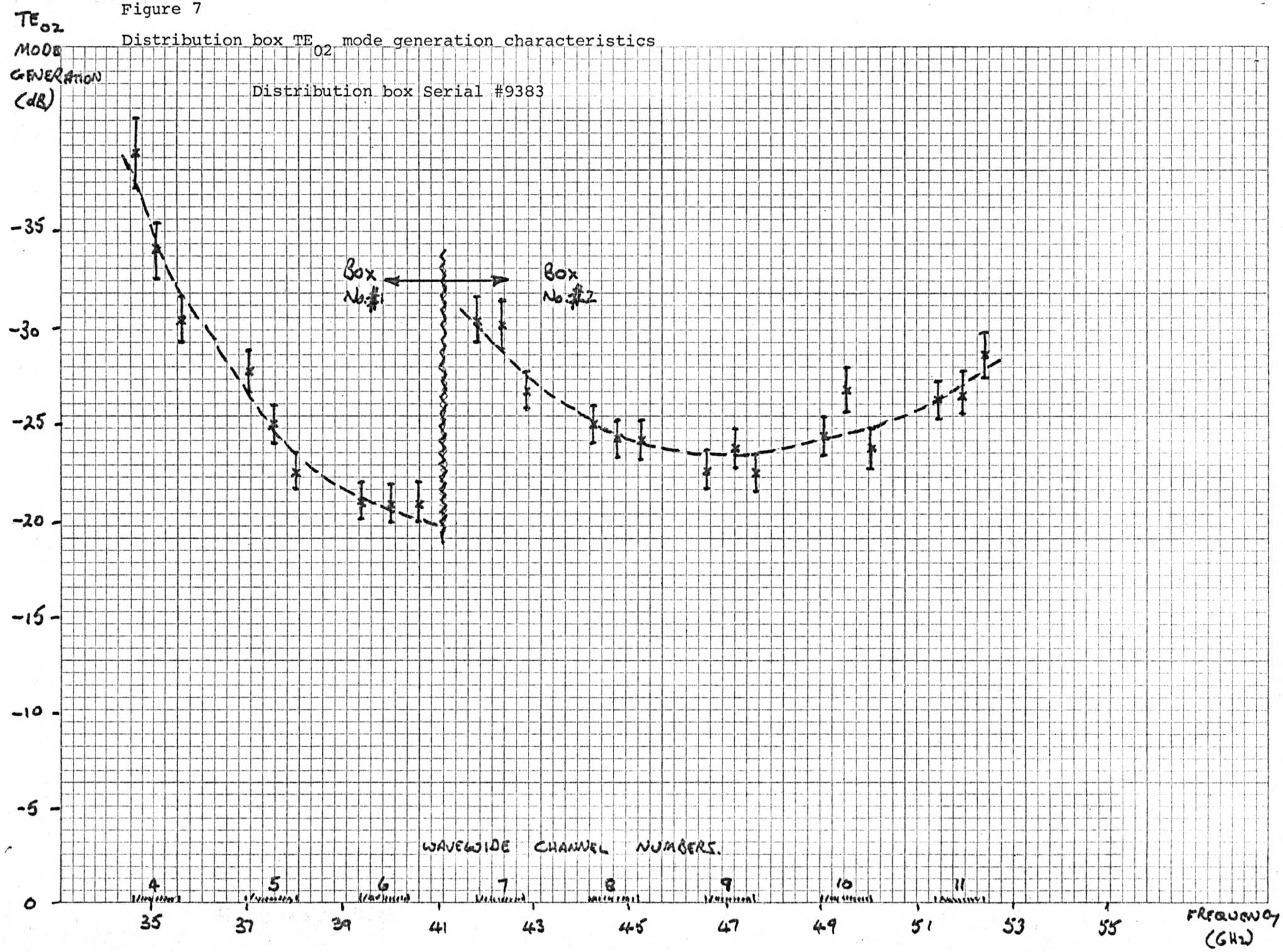

Figure 8(a)

Coupled arm TE_{02} mode generation for directional coupler with transition No. 1 (9.0" long)

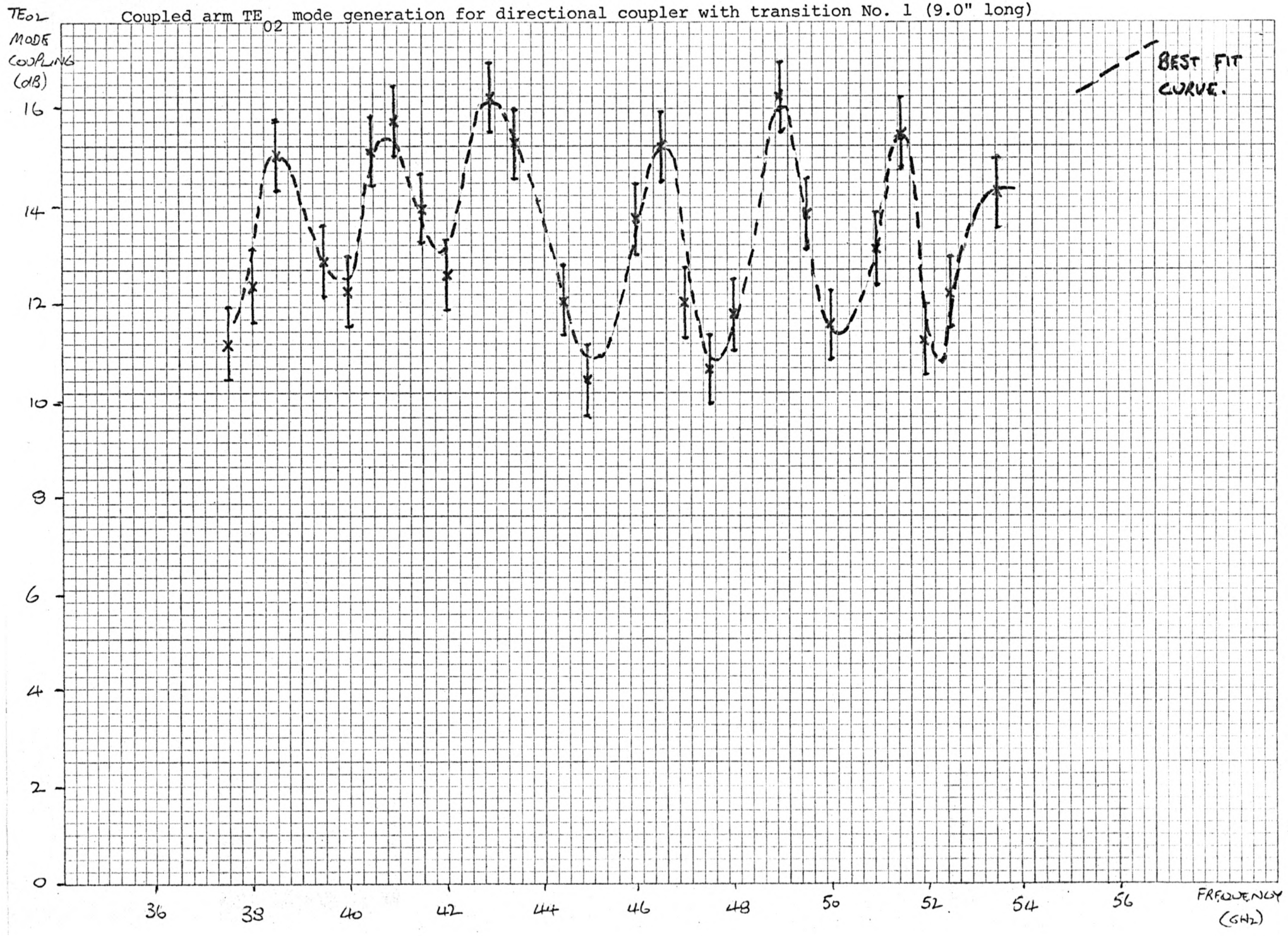

Figure 8 (b)

Coupled arm TE_{02} mode generation for directional coupler with transition No. 2 (4.5" long)

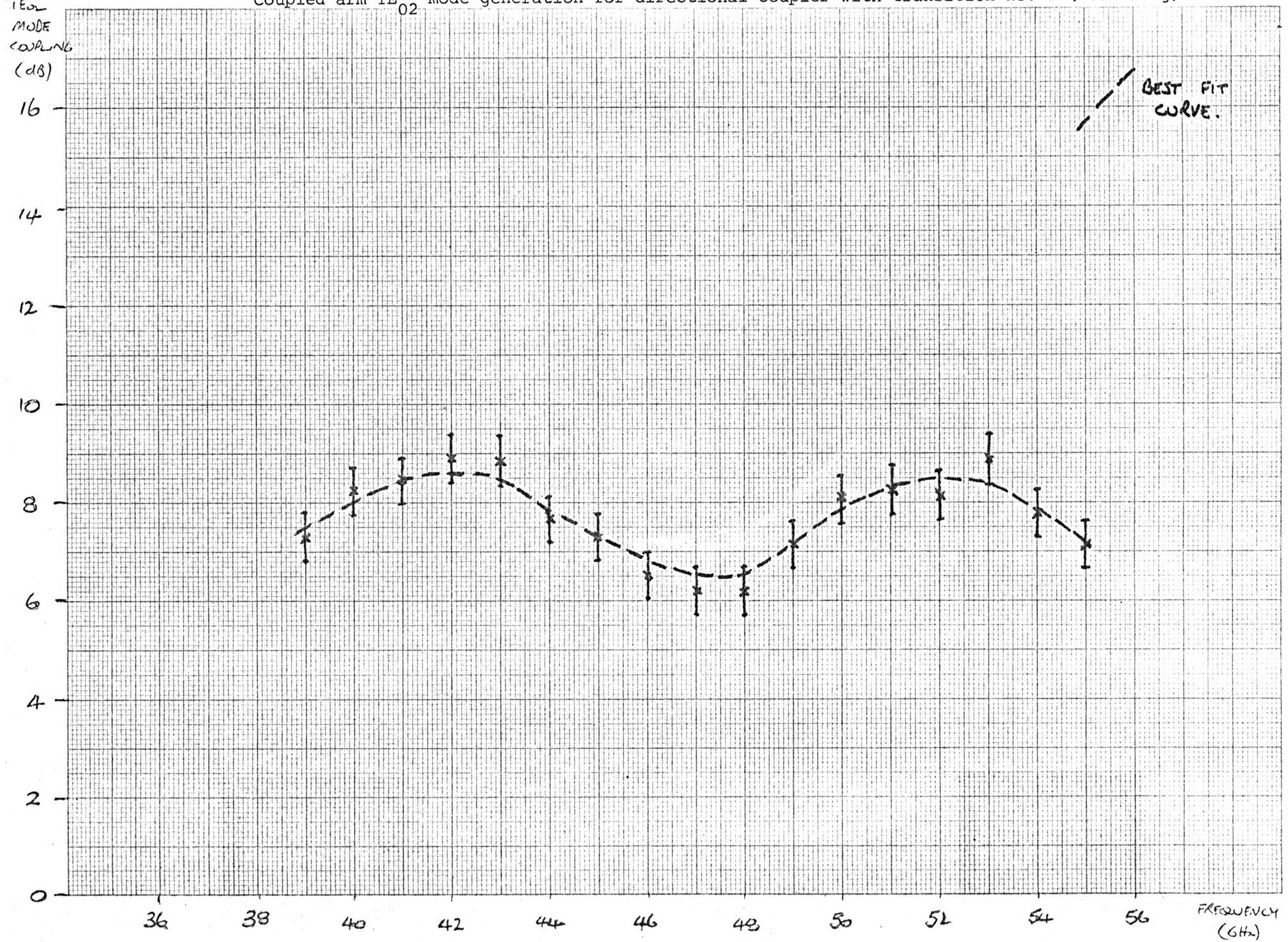

The level of coupler TE_{02} mode interaction depends upon the nature of the sector waveguide to circular waveguide transition (Archer et al. [1978]) in the coupled waveguide. Figures 8(a) and 8 (b) indicate the response for two types of transition. The variation in the coupler coupled arm response may be explained by considering a TE_{02} mode interaction between the sector mirror in the coupler body and the $180^{o} \rightarrow 360^{o}$ transition in the 60 mm diameter coupled waveguide arm. It can be seen that the use of the transition corresponding to the response of Figure 8(b) brings about a reduction in the average TE_{02} mode generation level and it is therefore advantageous to use this transition in all couplers installed in the VLA waveguide network.

The mode coupling performance of two typical waveguide tapers from 20 mm to 60 mm diameter when connected back-to-back was determined to be less than -40 dB over the frequency range 27 to 50 GHz. This coupling figure represents the measurement limit when using the above techniques and generators. Furthermore, when a typical production model sector coupler was connected between a pair of waveguide tapers and the main 60 mm diameter line mode coupling was determined (coupled port terminated), the TE_{02} mode conversion was found to be not greater than -38 dB over the same frequency range. Similar measurements on a Michelson interferometer type coupler (Iiguchi [1961]) indicated a main line mode conversion coefficient of approximately -20 dB at 30 GHz, -24 dB at 40 GHz and -25.5 dB at 50 GHz.

Figure 9 (a)

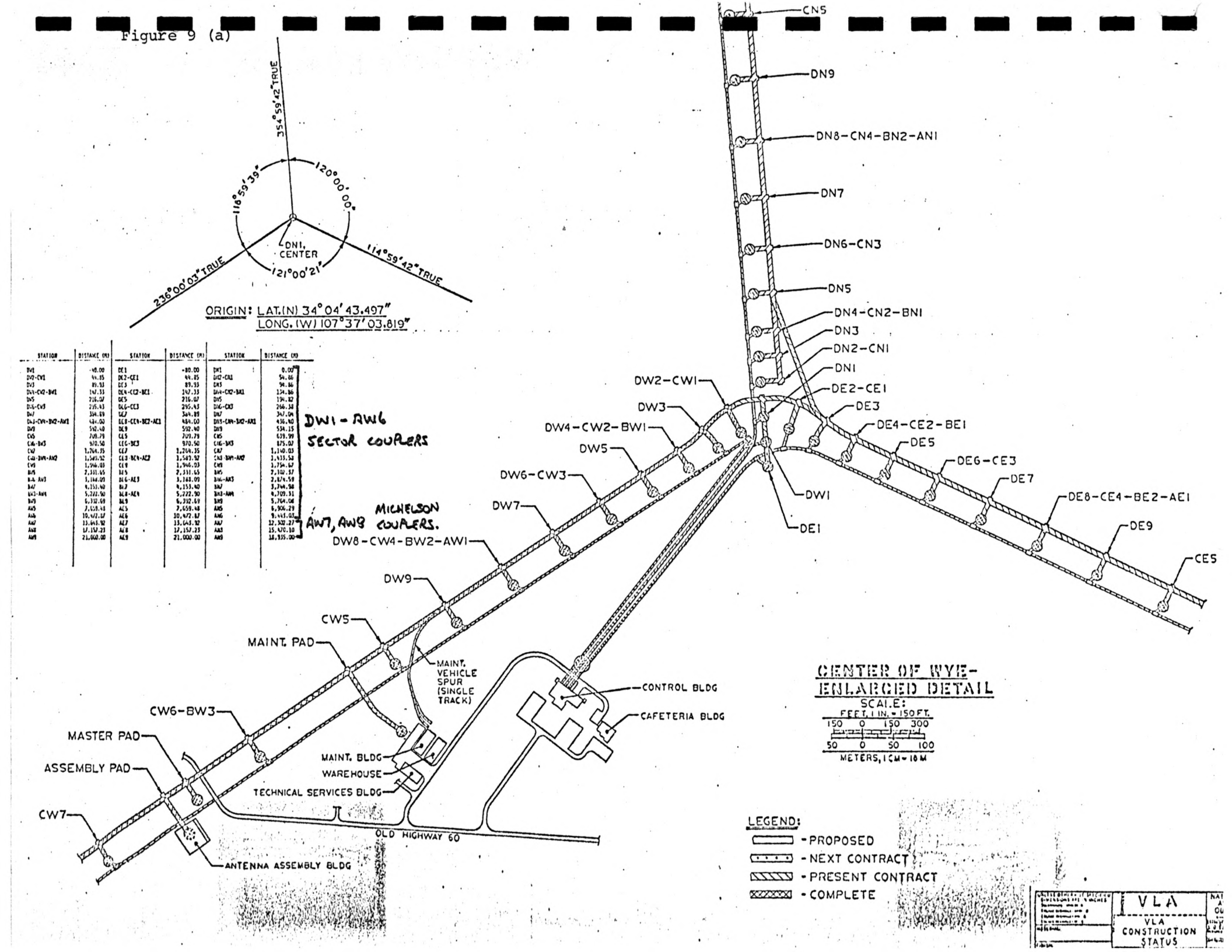

STATION	DISTANCE (M)	STATION	DISTANCE (M)	STATION	DISTANCE (M)
DW1	-80.00	DE1	+80.00	DN1	0.00
DW2-CW1	94.85	DE2-CE1	94.85	DN2-CN1	94.86
DW3	89.33	DE3	89.33	DN3	94.86
DW4-CW2-BW1	147.33	DE4-CE2-BE1	147.33	DN4-CN2-BN1	134.86
DW5	216.07	DE5	216.07	DN5	196.32
DW6-CW3	295.43	DE6-CE3	295.43	DN6-CN3	266.38
DW7	384.89	DE7	384.89	DN7	347.04
DW8-CW4-BW2-AW1	484.00	DE8-CE4-BE2-AE1	484.00	DN8-CN4-BN2-AN1	436.40
DW9	592.40	DE9	592.40	DN9	534.15
CW5	709.79	CE5	709.79	CN5	639.99
CW6-BW3	970.50	CE6-BE3	970.50	CN6-BN3	875.02
CW7	1,264.35	CE7	1,264.35	CN7	1,140.03
CW8-BW4-AW2	1,569.92	CE8-BE4-AE2	1,569.92	CN8-BW4-AW2	1,435.58
CW9	1,946.03	CE9	1,946.03	CW9	1,794.67
BW5	2,331.65	BE5	2,331.65	BW5	2,102.37
BW6-AW3	3,144.09	BE6-AE3	3,168.09	BW6-AW3	2,874.59
BW7	4,153.40	BE7	4,153.40	BW7	3,744.98
BW8-AW4	5,222.90	BE8-AE4	5,222.90	BW8-AW4	4,709.51
BW9	6,332.69	BE9	6,332.69	BW9	5,764.06
AW5	7,659.48	AE5	7,659.48	AW5	6,906.29
AW6	10,472.87	AE6	10,472.87	AW6	9,445.03
AW7	13,645.92	AE7	13,645.92	AW7	12,302.27
AW8	17,157.23	AE8	17,157.23	AW8	15,470.10
AW9	21,000.00	AE9	21,000.00	AW9	18,935.00

CENTER OF WYE-ENLARGED DETAIL

SCALE:
FEET, 1 IN. = 150 FT.
150 0 150 300
50 0 50 100
METERS, 1 CM = 10 M

LEGEND:
- PROPOSED
- NEXT CONTRACT
- PRESENT CONTRACT
- COMPLETE

VLA
VLA CONSTRUCTION STATUS

Figure 3 (b)

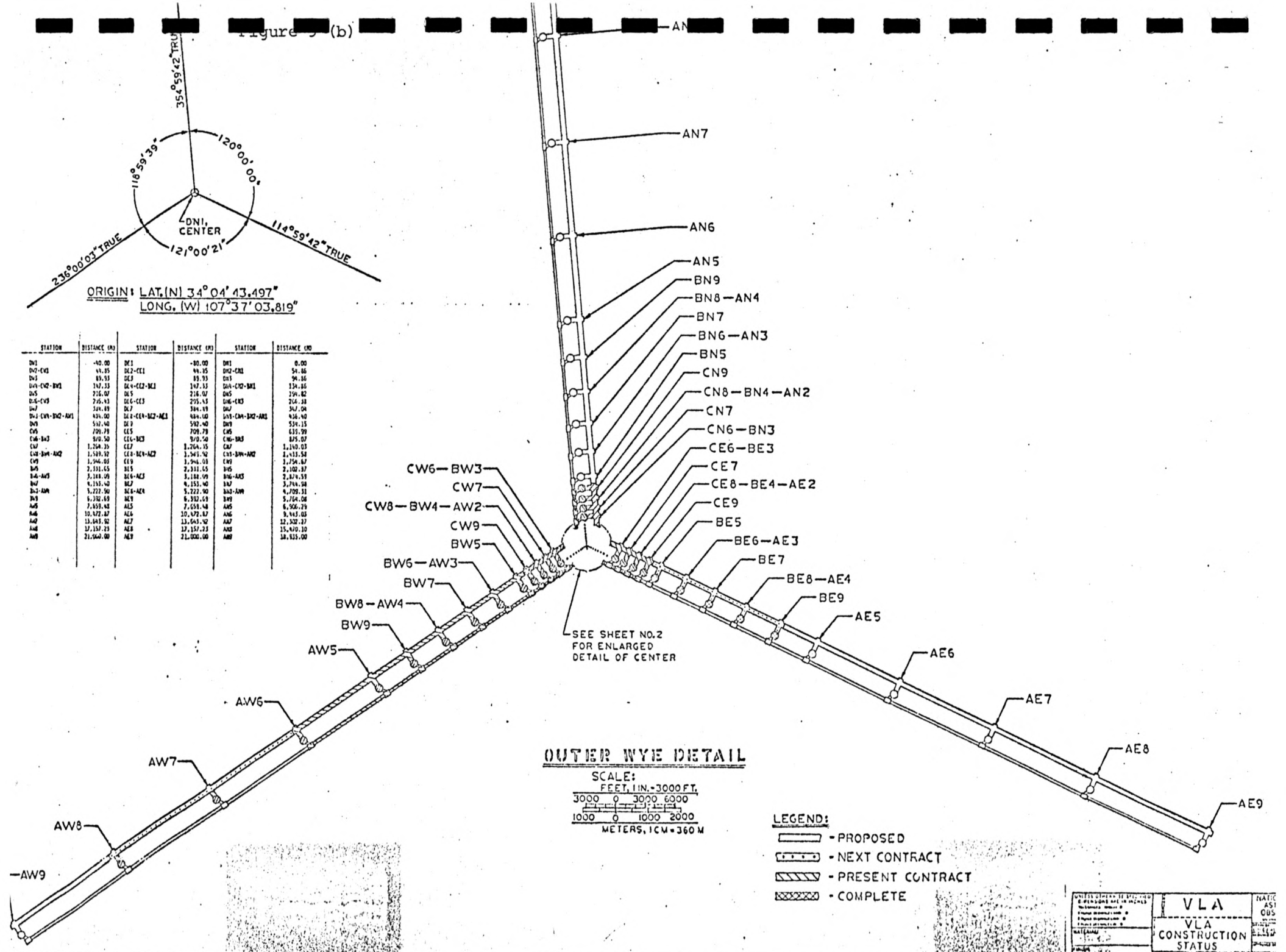

ORIGIN: LAT. (N) 34° 04' 43.497"
LONG. (W) 107° 37' 03.819"

STATION	DISTANCE (M)	STATION	DISTANCE (M)	STATION	DISTANCE (M)
DN1	-40.00	DE1	-80.00	DW1	0.00
DN2-CN1	44.85	DE2-CE1	44.85	DW2-CW1	54.86
DN3	89.53	DE3	89.53	DW3	94.86
DN4-CN2-BN1	147.33	DE4-CE2-BE1	147.33	DW4-CW2-BW1	154.86
DN5	216.07	DE5	216.07	DW5	194.82
DN6-CN3	295.43	DE6-CE3	295.43	DW6-CW3	236.68
DN7	384.89	DE7	384.89	DW7	347.04
DN8-CN4-BN2-AN1	484.00	DE8-CE4-BE2-AE1	484.00	DW8-CW4-BW2-AW1	436.40
DN9	592.40	DE9	592.40	DW9	534.15
CN5	709.79	CE5	709.79	CW5	635.99
CN6-BN3	840.50	CE6-BE3	840.50	CW6-BW3	825.07
CN7	1,264.35	CE7	1,264.35	CW7	1,140.03
CN8-BN4-AN2	1,549.92	CE8-BE4-AE2	1,549.92	CW8-BW4-AW2	1,433.58
CN9	1,946.08	CE9	1,946.08	CW9	1,754.67
BE5	2,311.65	BE5	2,311.65	BW5	2,102.87
BE6-AE3	3,188.09	BE6-AE3	3,188.09	BW6-AW3	2,874.59
BE7	4,155.40	BE7	4,155.40	BW7	3,744.98
BE8-AE4	5,222.90	BE8-AE4	5,222.90	BW8-AW4	4,709.31
BE9	6,392.69	BE9	6,392.69	BW9	5,764.08
AE5	7,658.48	AE5	7,658.48	AW5	6,906.29
AE6	10,472.87	AE6	10,472.87	AW6	9,443.03
AE7	13,643.92	AE7	13,643.92	AW7	12,532.27
AE8	17,157.23	AE8	17,157.23	AW8	15,470.10
AE9	21,060.00	AE9	21,000.00	AW9	18,535.00

OUTER WYE DETAIL

SCALE:
FEET, 1 IN. = 3000 FT.
3000 0 3000 6000
1000 0 1000 2000
METERS, 1 CM = 360 M

LEGEND:
- PROPOSED
- NEXT CONTRACT
- PRESENT CONTRACT
- COMPLETE

VLA
VLA CONSTRUCTION STATUS

Finally, the mode conversion coefficient of the rectangular-to-circular adapter used at each modem input at the antennas was found typically to be less than -35 dB for any waveguide channel in the frequency range 27-51 GHz in which the adapter was specified to operate.

5.0 PREDICTION AND MEASUREMENT OF THE VARIATION IN THE TE_{01} MODE TRANSMISSION FUNCTION

5.1 Predicted Variations Caused by Reflections

The typical measured data given in Table 1 for the TE_{01} mode performance of the coupler, main waveguide, distribution box and tapers can be substituted in equation (3.8) to derive an estimate of the mean square ripple in the transmission response at a given station due to TE_{01} mode reflections in the main waveguide. Furthermore, an estimate of the power spectrum of the ripple in terms of the interaction length scale size (which determines the ripple period at a given frequency) can be derived at each station. Figure 10 shows the predicted mean square deviation of the transfer function from the uniform response expected, in the presence of waveguide attenuation alone, at the coupler output at each antenna station on the southwest arm of the array (couplers installed at every station as indicated in Figure 9). Figure 11 presents the ripple power spectrum (due to reflection interactions) at selected stations on the southwest arm.

Figure 10

Mean square variation in TE_{01} transfer function due to reflections

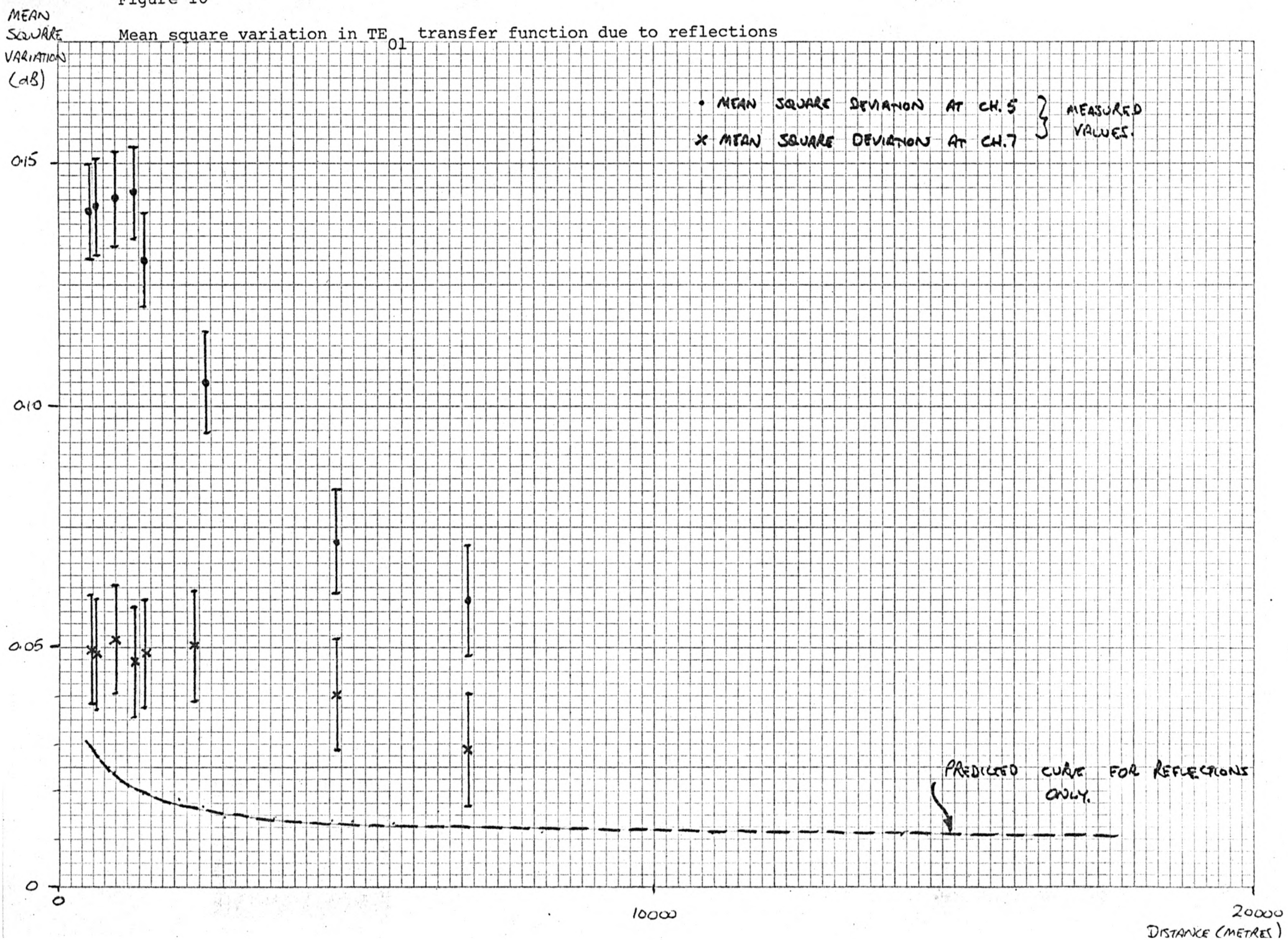

Figure 11 (a)

Power spectrum of TE_{01} mode transmission function variation predicted at DW2 due to reflections

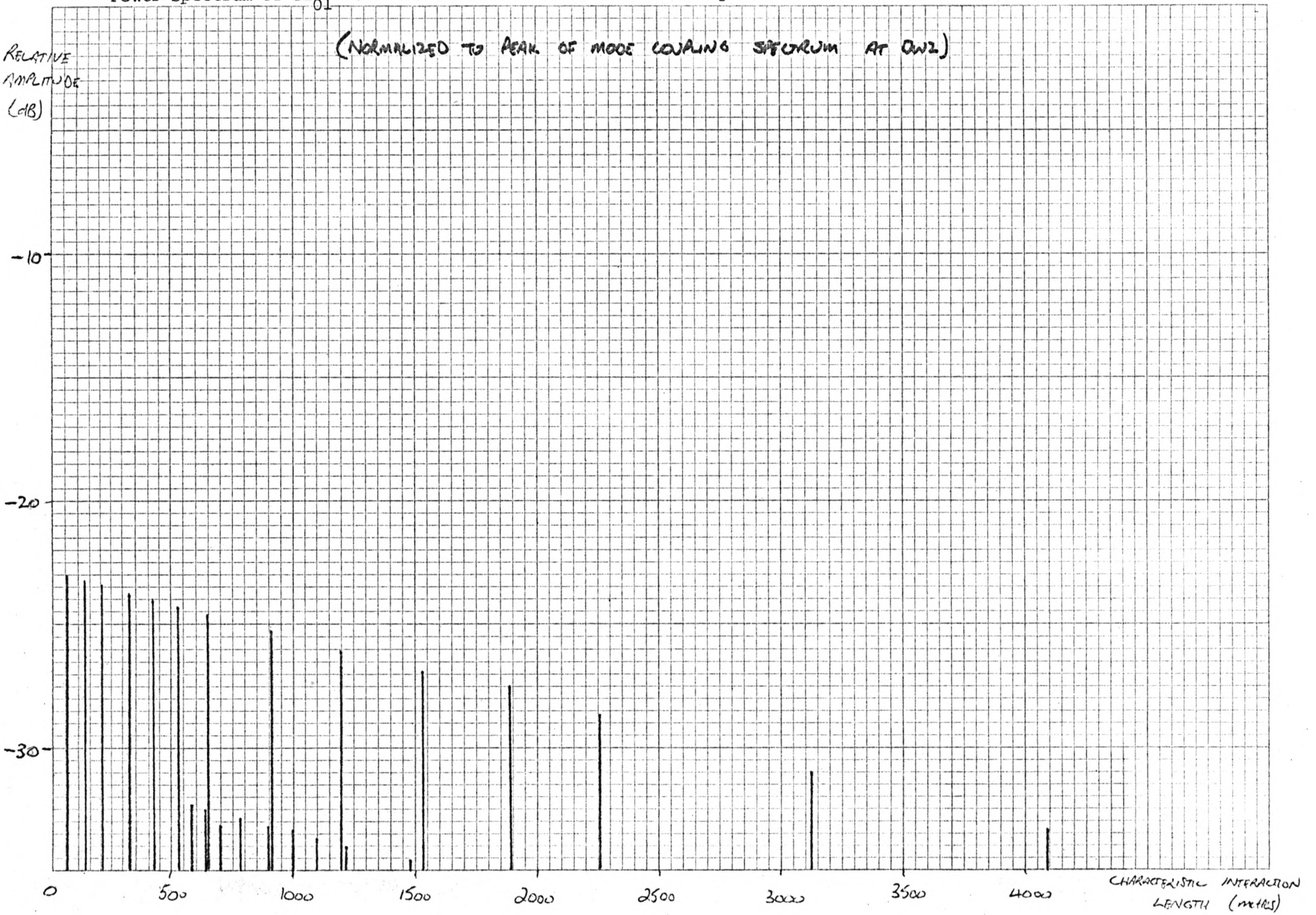

Figure 11 (b)

Power spectrum of TE_{01} mode transmission function variation predicted at BW 7 due to reflections

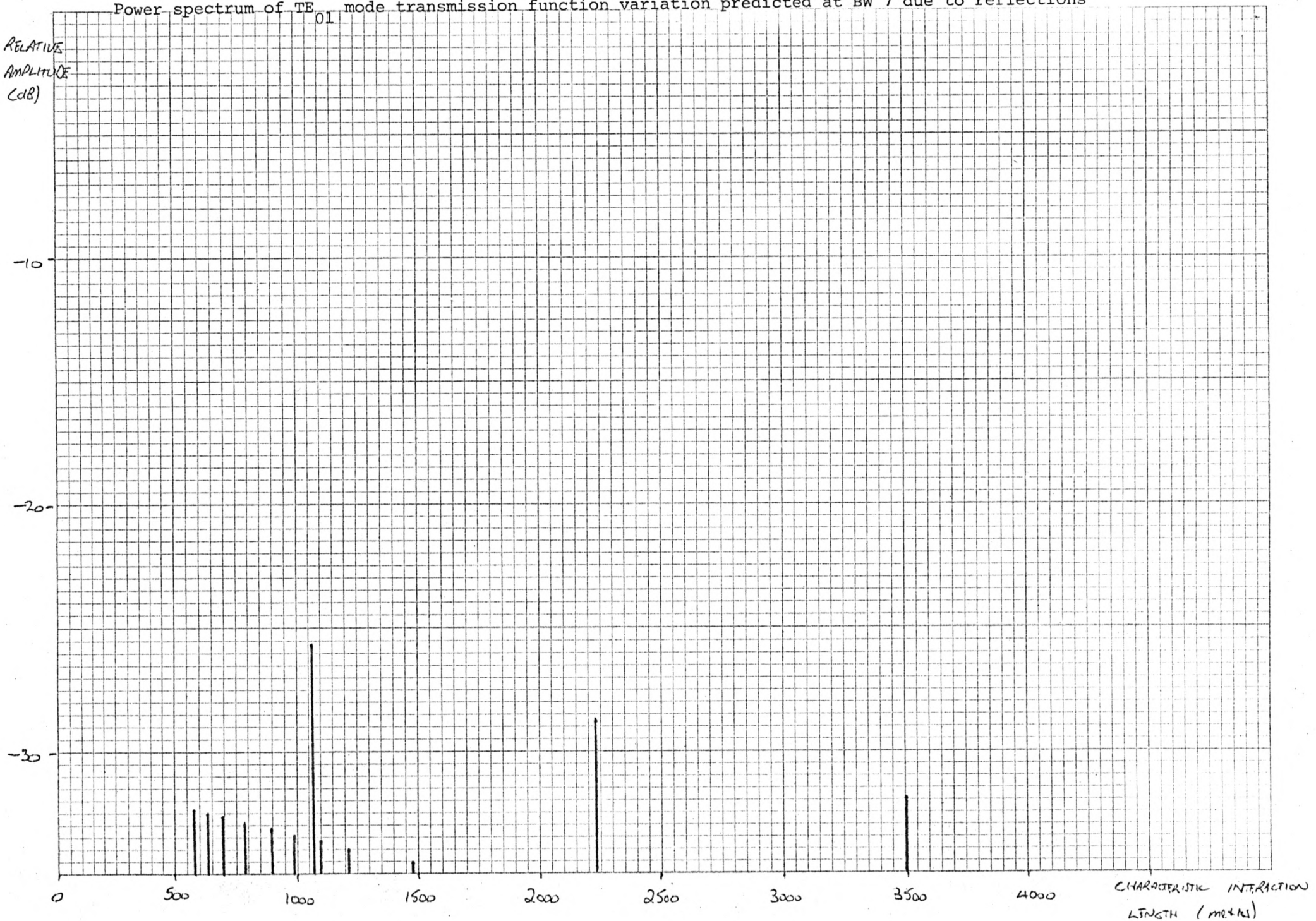

In most cases the expected ripple amplitude is seen to be such that it would not be readily detectable by routine swept frequency transmission loss measurements and is in all cases less than a mean square value of 0.05 dB, the specified tolerable level for small scale frequency dependent perturbations. Furthermore, the maximum expected mean square variation in antenna waveguide transmission response due to reflective interactions between the coupler and the modem is 0.02 dB.

5.2 Predicted Variations Caused by Mode Conversions

By applying the data given in Figures 7 and 8 to equation (3.7), the best and worst case ripple in the TE_{01} mode transmission response due to TE_{02} mode conversion-reconversion effects can be derived. The worst case condition is taken to be that frequency at which the coupler main to coupled arm and distribution box mode conversion coefficients are at a maximum. Figure 12 shows the best and worst case predicted mean square deviation of the TE_{01} mode transfer function from the uniform response, expected in the presence of waveguide attenuation and perfect couplers alone, at each coupler output on the southwest arm of the array. Figure 13 indicates the predicted ripple power spectrum (due to mode conversion-reconversion) at selected stations on the same arm. Both figures are plotted for the case where couplers are installed at every station on the southwest arm.

Figure 12

Mean square variation in TE_{01} transfer function due to mode coupling

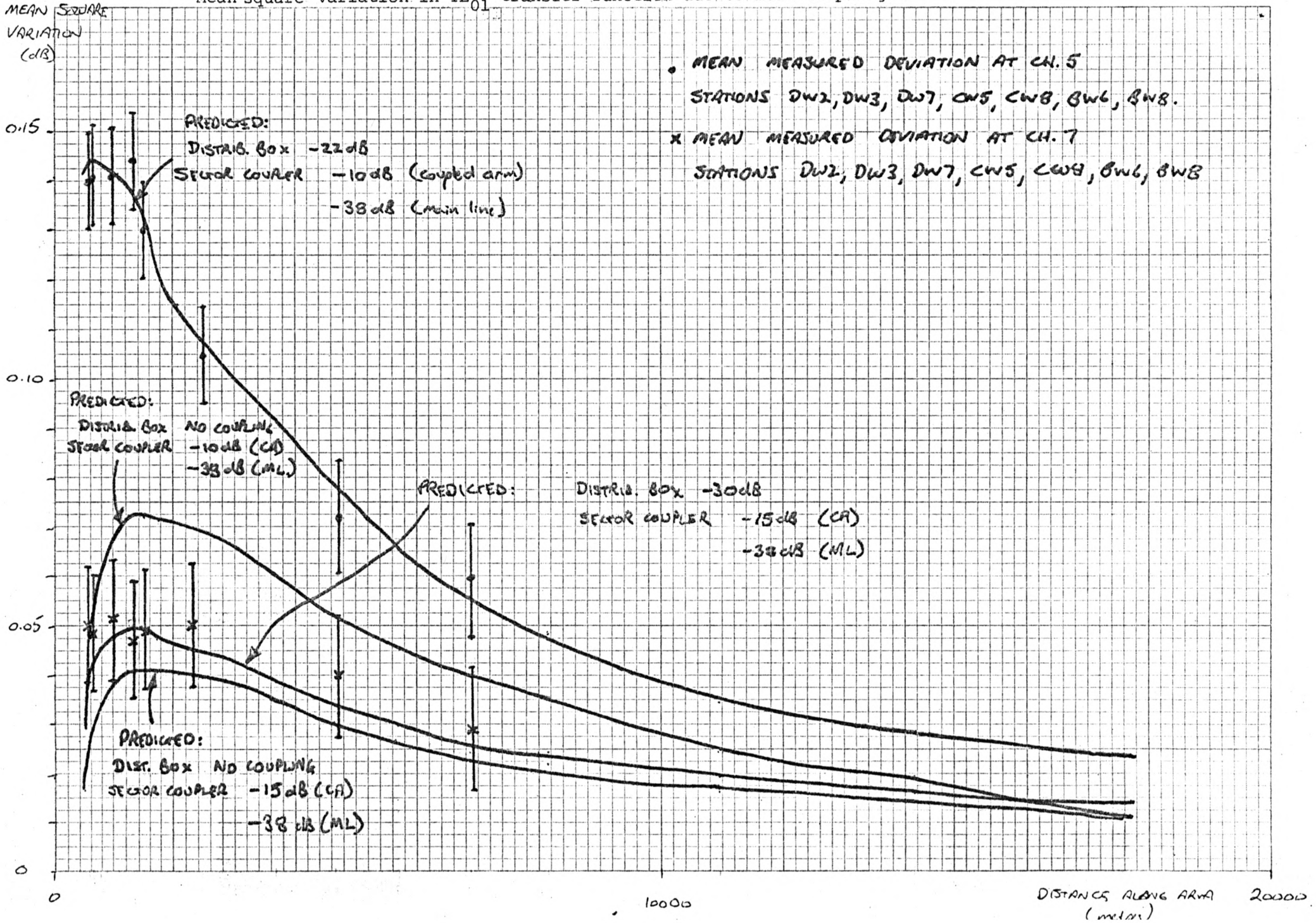

It can be seen that the worst case expected mean square ripple amplitude is greater than 0.05 dB for all stations within approximately 2.5 km of the distribution box. Furthermore, reducing the distribution box mode conversion coefficient while holding all other parameters constant results in a reduction of the ripple at stations near the center of the array, as indicated in Figure 12, while not altering significantly the behavior at remote antennas. It is expected, therefore, that the significant contribution to the TE_{01} mode transmission function ripple should arise from interactions between the distribution box and couplers within 2.5 km of the array center.

With reference to the antenna waveguide, TE_{02} mode interactions between the coupler and the rectangular-to-circular waveguide adapter would be expected to result in a worst case mean square TE_{01} mode transmission variation of less than 0.02 dB. No other TE_{02} mode conversion-reconversion sources should occur in the 20 mm diameter antenna waveguide.

5.3 Measurements of the TE_{01} Mode Transmission Function Variation on the Southwest Arm

The mean square variation in the TE_{01} mode transmission characteristics at selected stations on the southwest arm of the VLA waveguide system has been determined by direct swept frequency measurements in waveguide channels 5 and 7. These channels correspond approximately to the worst and best case

coupler performance respectively. The typical measured mean square ripple at channel center frequency is plotted as a function of distance along the arm, for comparison with the predicted results, in Figures 12 and 10. These measurements were made with a power-levelled sweep frequency signal generator connected to the channel 5 or 7 rectangular waveguide port of the distribution box and a power sensor connected to the required coupler coupled arm via a waveguide taper and a rectangular-to-circular transition. The power sensor comprised a square law crystal detector and DC amplifier connected to the coupled port of a terminated rectangular waveguide -10 dB directional coupler. The minimum detectable power level was -40 dBm and the sensor return loss was greater than 35 dB. Close similarity between the measured points and the TE_{02} mode conversion-reconversion plot of Figure 12 is noted, especially near the array center. The well defined ripple period measured at the close in stations suggested a TE_{02} mode interaction between the couplers and a component near the control building. The second set of points in Figures 12 and 10, indicates the measured mean square variation in the TE_{01} mode transmission function when the distribution box is bypassed and the signal fed directly from the signal generator into the waveguide network. Clearly, the TE_{01} mode ripple at the stations close to the array center is significantly reduced. It would appear desirable, therefore, to either introduce a TE_{02} mode filter after the

distribution box or to improve the coupler mode conversion characteristics in order to achieve the TE_{01} mode transfer function variation specification at the close in stations.

Measurements have also been made, in a number of cases, of the additional TE_{01} mode ripple introduced when the antenna waveguide is included in the signal path. In general, the increase in mean square ripple amplitude is found not to be significant when the antenna waveguide has been properly installed. Several cases of serious performance degradation have, however, been noted. All of these antennas have been found to have damaged or poorly installed flexible waveguide sections which gave rise to excessive TE_{02} mode interaction with the directional coupler.

6.0 A TE_{on} MODE FILTER FOR THE VLA WAVEGUIDE SYSTEM

Coupler interactions within the sector waveguide to circular waveguide transition of the sector coupler make it difficult to predict in a rational theoretical manner the effects of modifying the profile of the expansion taper, the sector mirror shape or angle or the taper length. The most straightforward method for reducing the magnitude of the variation in the TE_{01} mode transmission function at stations close to the center of the array is, therefore, to insert a TE_{on} mode filter in the 20 mm diameter waveguide line connecting distribution box to the main 60 mm diameter trunk waveguide line. Since it seems

Figure 13 (a)

Power spectrum of TE_{01} mode transmission function variations predicted at DW2 due to mode coupling

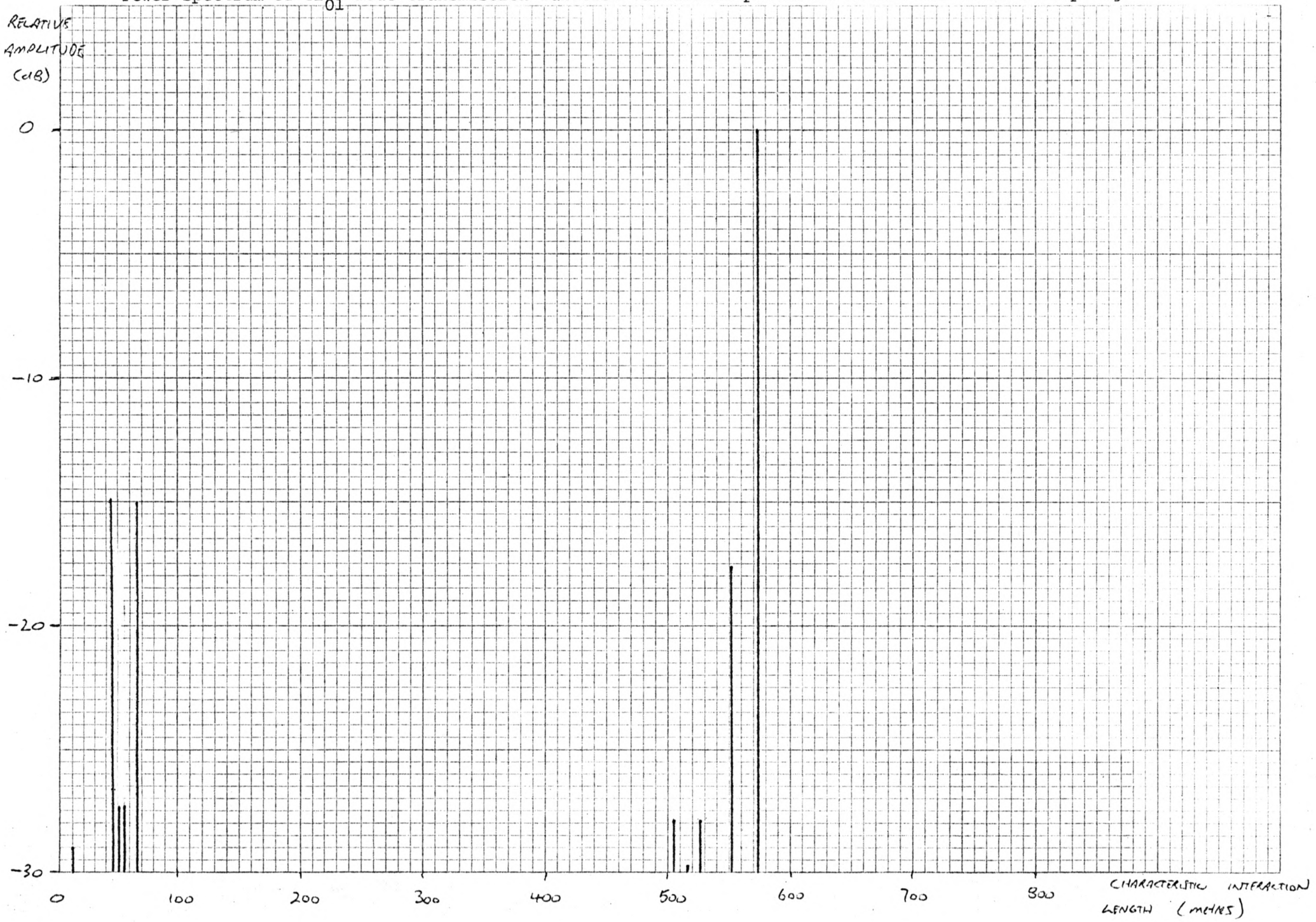

Figure 13 (b)

Power spectrum of TE_{01} mode transmission function variations predicted at DW 2 due to mode coupling

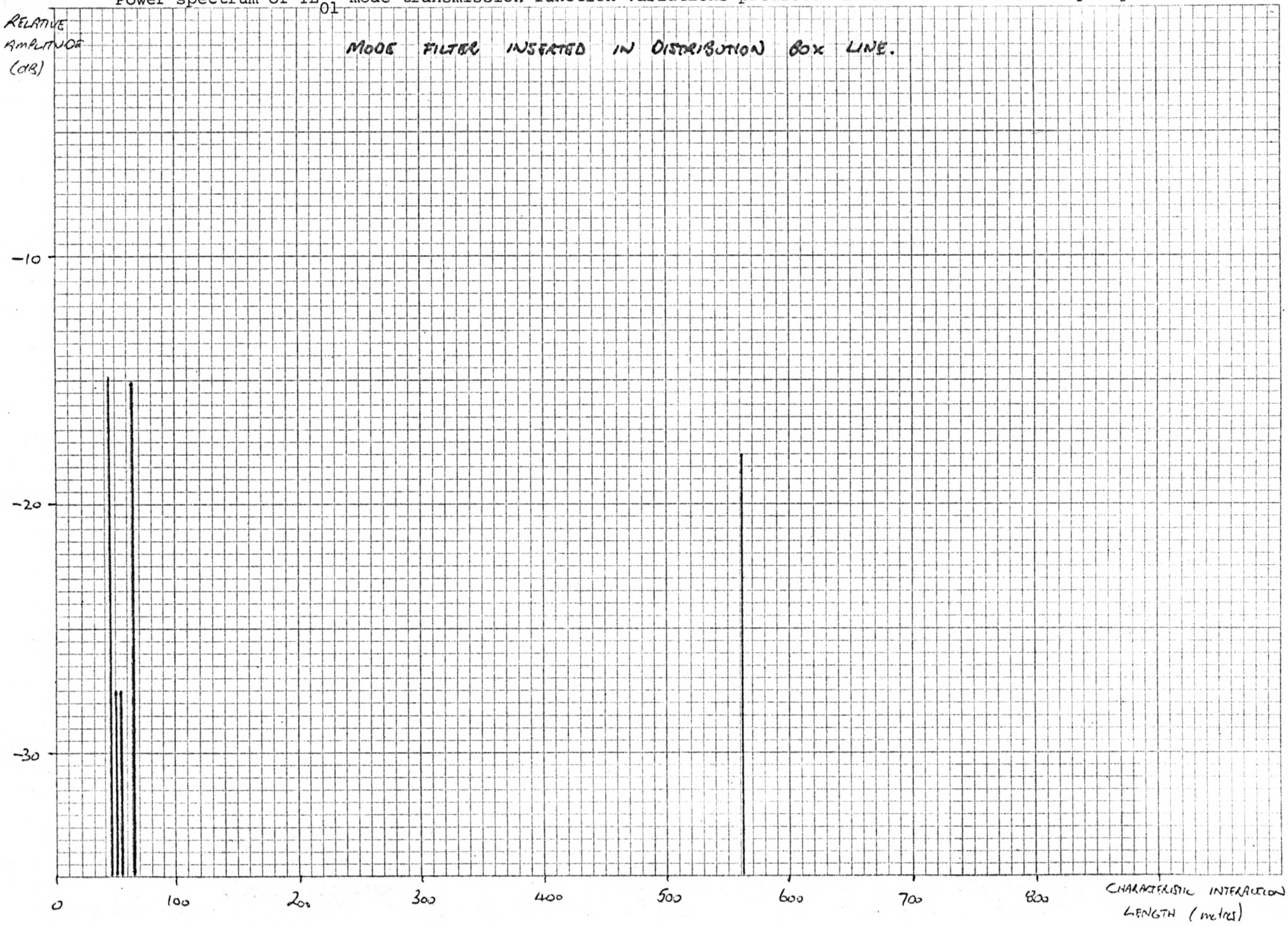

Figure 13 (c)

Power spectrum of TE_{01} mode transmission function variations predicted at CW6 due to mode coupling

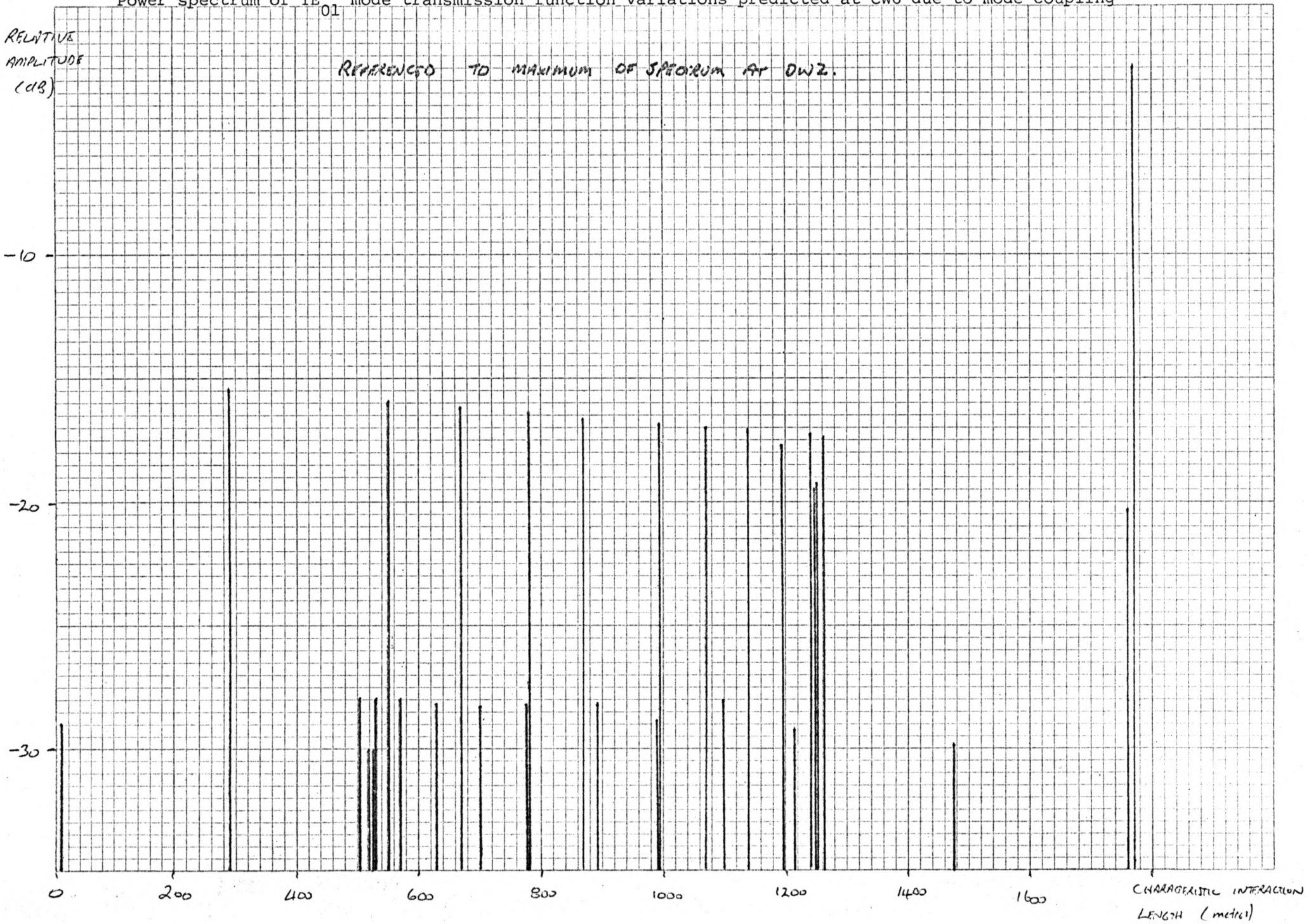

Figure 13 (d)

Power spectrum of TE_{01} mode transmission function variations predicted at CW6 due to mode coupling

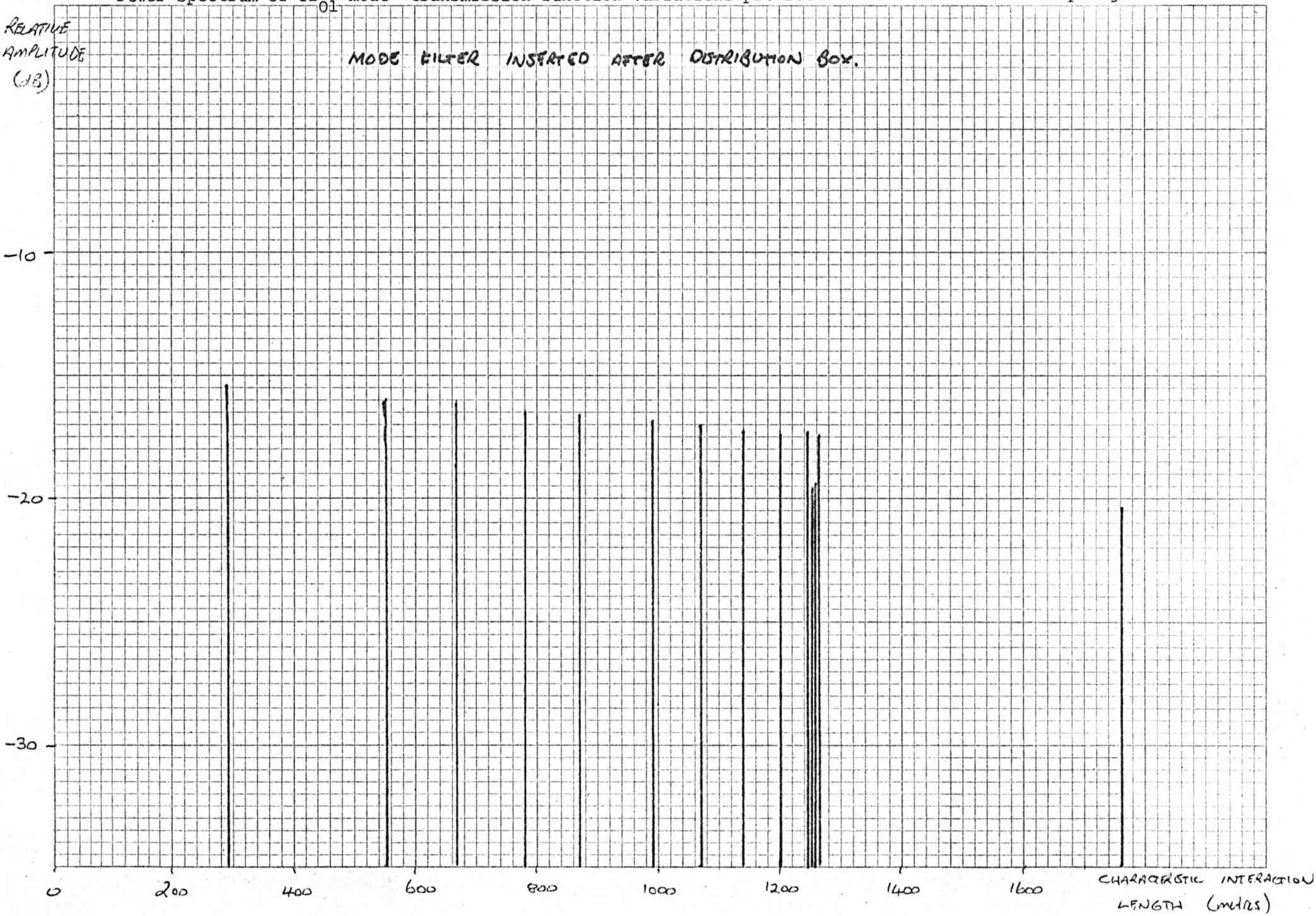

Figure 13 (e)

Power spectrum of TE_{01} mode transmission function variations predicted at BW7 due to mode coupling

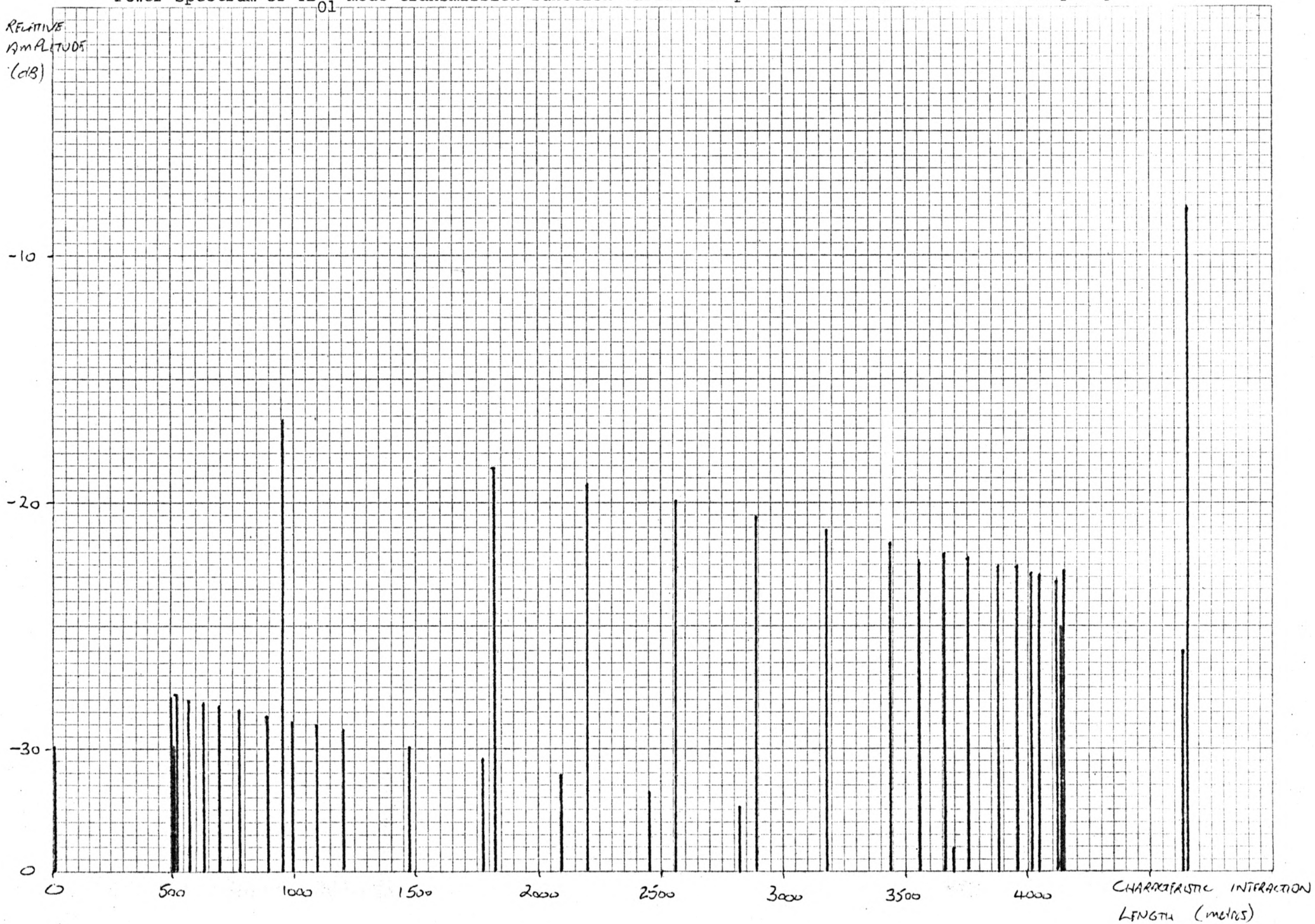

Figure 13 (f)

Power spectrum of TE_{01} mode transmission function variations predicted at AW7 due to mode coupling

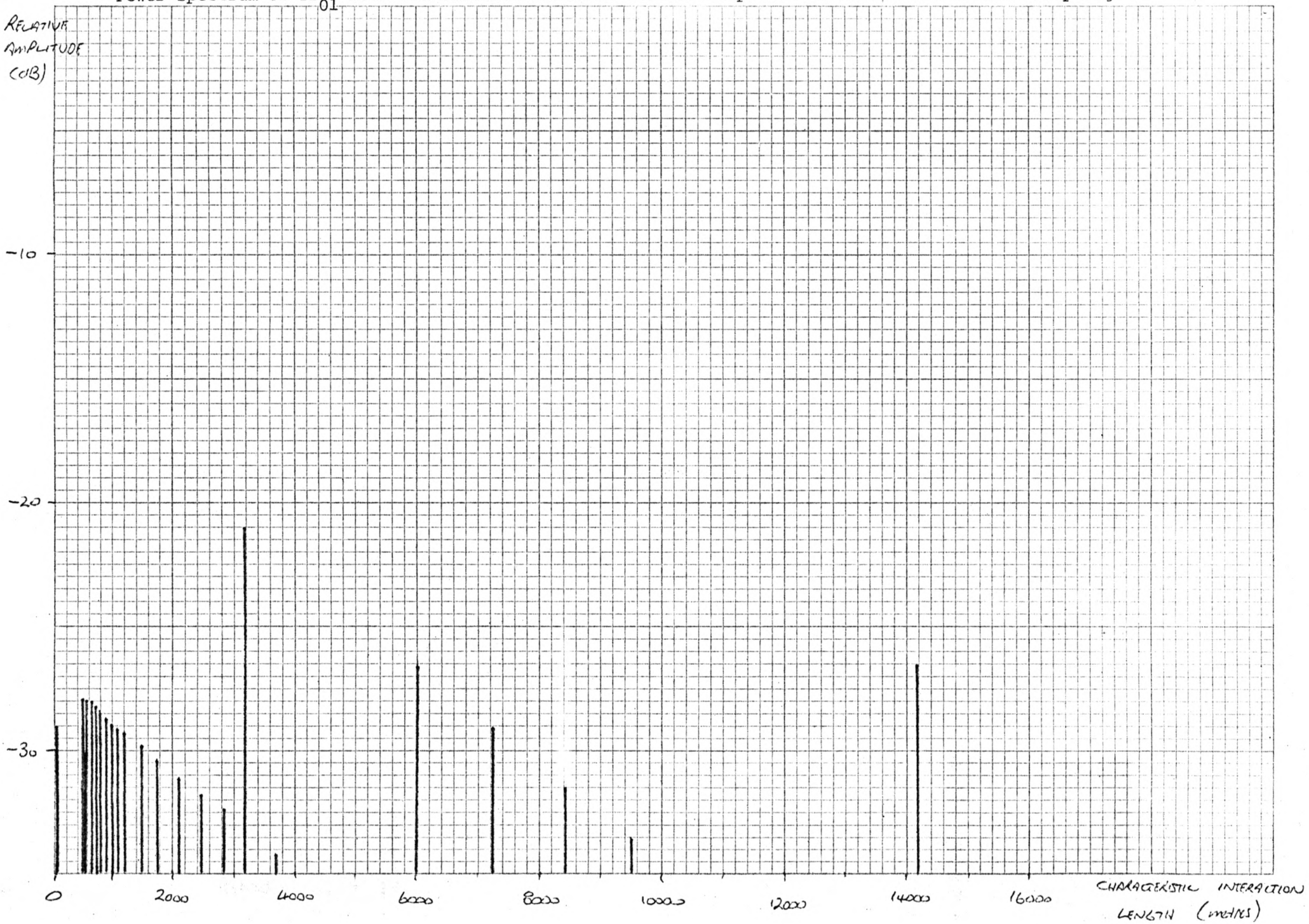

most probable that waveguide channels 1 through 9 (27.4 to 47.6 GHz) will be used as the operational frequencies, with channels 10 and 11 as spares, it is sufficient for the filter to attenuate strongly the TE_{02} mode and all higher order circular electric modes for frequencies below 47.6 GHz and to transmit with low loss the TE_{01} mode for all frequencies above 27.4 GHz.

A number of coupler TE_{on} mode filter designs are currently available including helix-waveguide polygonal deformation (Inada, et al [1973]) and multi-sector phase dispersion types (Powell, et al [1976]). Polygonal type filters are narrow-band, with a -10 dB TE_{02} mode rejection bandwidth of at best 20% of the center frequency for maximum TE_{0n} mode attenuation. Furthermore, they exhibit poor higher-order circular electric mode rejection at the design TE_{02} center frequency. Multi-sector phase dispersion filters, although theoretically capable of broadband TE_{02} mode rejection, have not been successfully fabricated commercially.

A much simpler filter design, shown in Figure 14, has been developed for the VLA waveguide system. This device uses the well known properties of cut-off waveguide to implement a filter which has high attenuation for all TE_{on} modes ($n > 1$) for frequencies below 47.853 GHz, yet transmits the TE_{01} mode with low loss for all frequencies above 26.136 GHz. The resultant channel guard bandwidths are, for the TE_{01} mode, 1.274 GHz, and for the TE_{02} mode, 243 MHz. The diameter

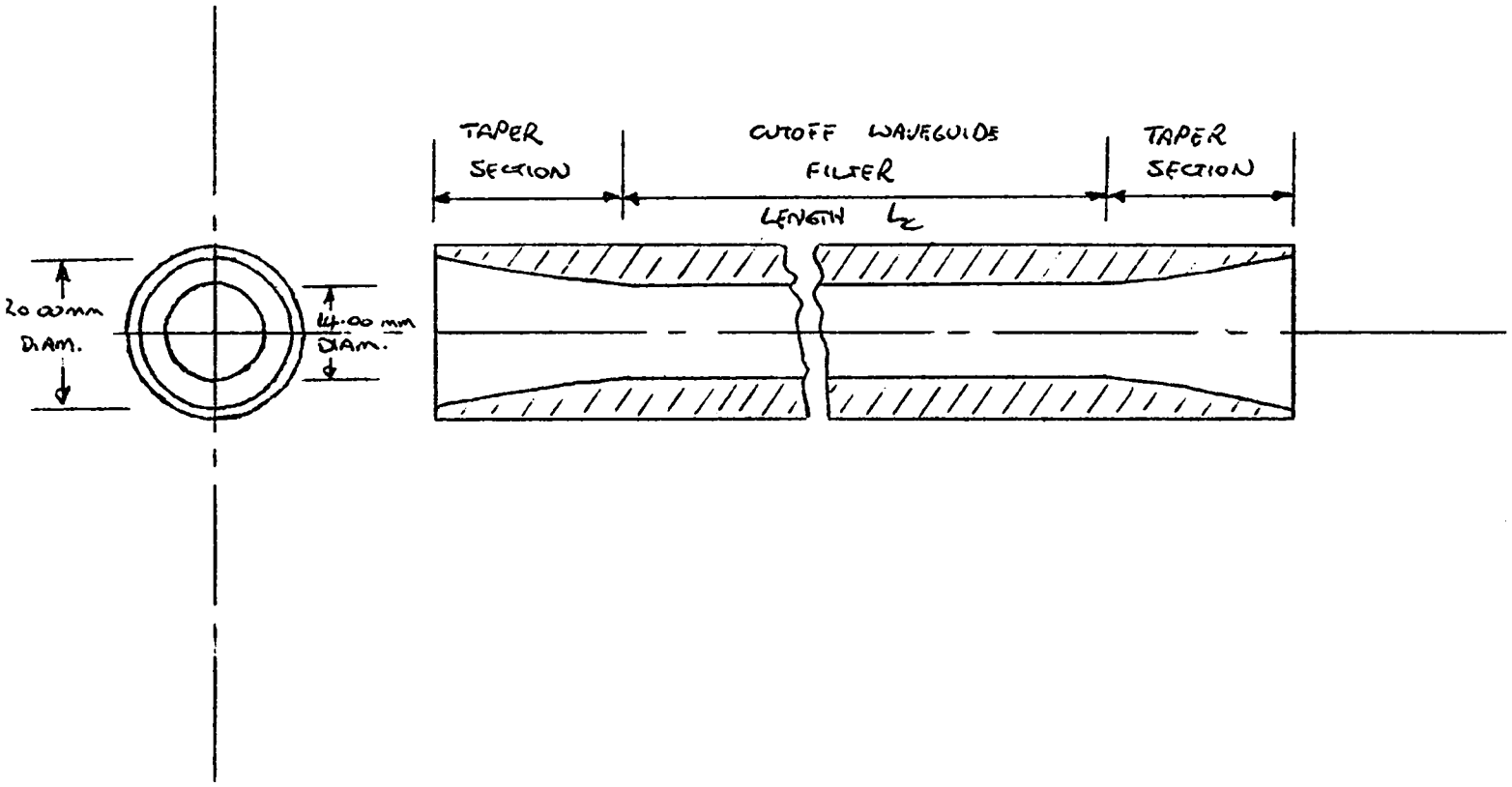

Figure 14

20 mm diameter circular waveguide TE_{On} mode filter (n>1)

of the cut-off waveguide section required to achieve this response is 14.00 mm. The theoretical TE_{01} and TE_{02} mode insertion losses are given by the expressions, for copper waveguide,

$$\alpha_{TE_{01}} \sim \frac{6.976 \times 10^{-7}}{a} \left[\frac{f_o}{\sqrt{1-\left(\frac{f_{co}}{f_o}\right)^2}} \right]^{\frac{1}{2}} \left(\frac{f_{co}}{f_o}\right)^2 \text{ Nepers/metre}$$

$$\alpha_{TE_{02}} \gtrsim \frac{2\pi}{\lambda_o} \left[\left(\frac{\lambda_o}{0.0895a}\right)^2 - 1 \right]^{\frac{1}{2}} \text{ Nepers/metre} \qquad (6.1)$$

where a is the waveguide radius,

f_o, λ_o are the operating frequency and wavelength respectively,

f_{co} is the cutoff frequency in the waveguide section.

The theoretical response is plotted in Figure 15 for a total waveguide length of 100.00 mm.

Two important considerations in the design of a filter of this type in the present application are, firstly, that the device must not, itself, couple significant power to higher order modes. Secondly, the filter must not introduce appreciable non-linear phase distortion in any of the IF bands transmitted by the waveguide network. The first consideration requires that the waveguide tapers from 14.00 mm to 20.00 mm diameter be carefully designed for minimum mode coupling over the desired operating frequency range. The theoretical approach used in the design of the waveguide tapers incorporated in the mode

Figure 15 (a)

Predicted TE_{01} mode insertion loss for mode filter

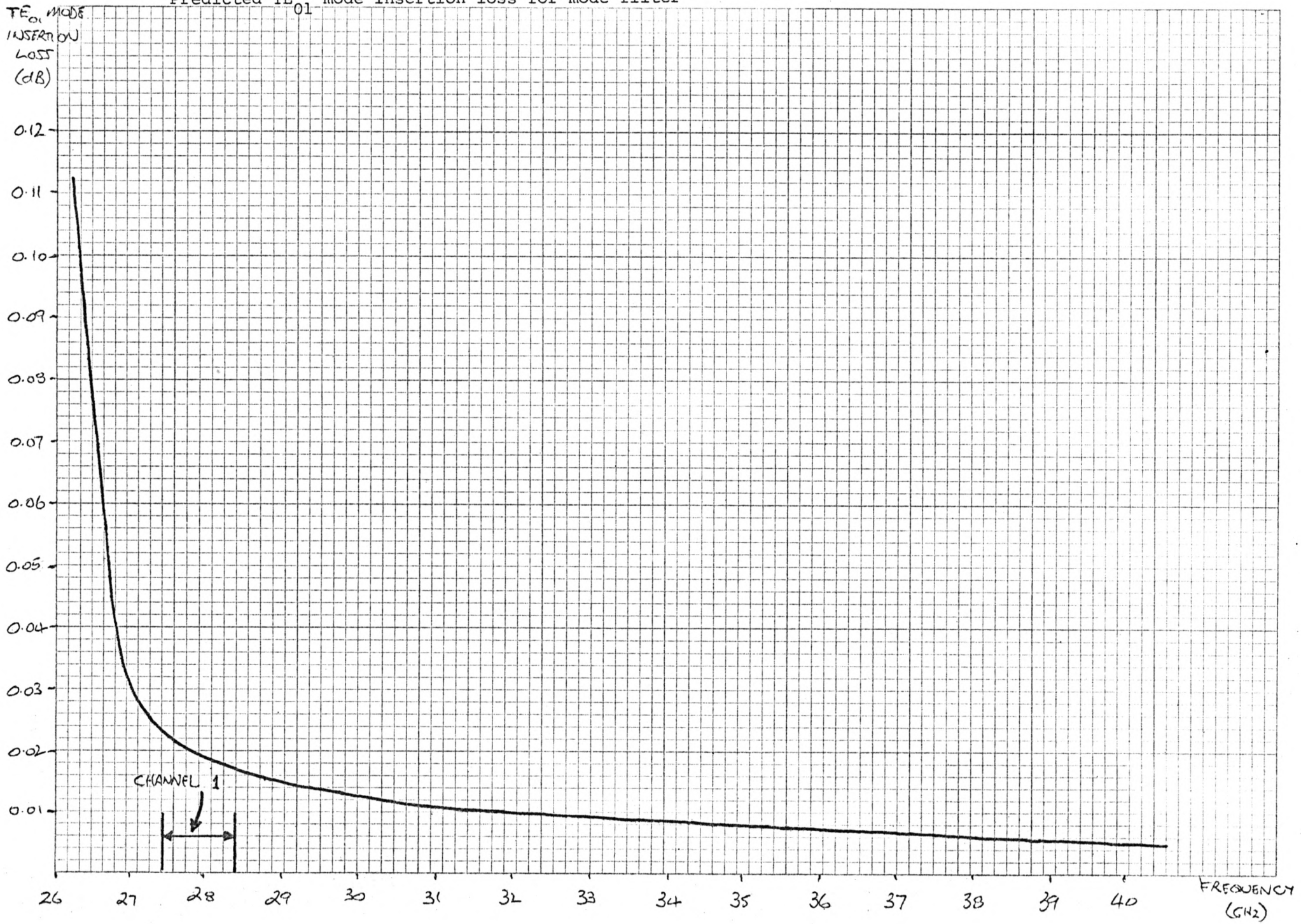

Figure 15 (b)

Predicted TE_{02} mode rejection for mode filter

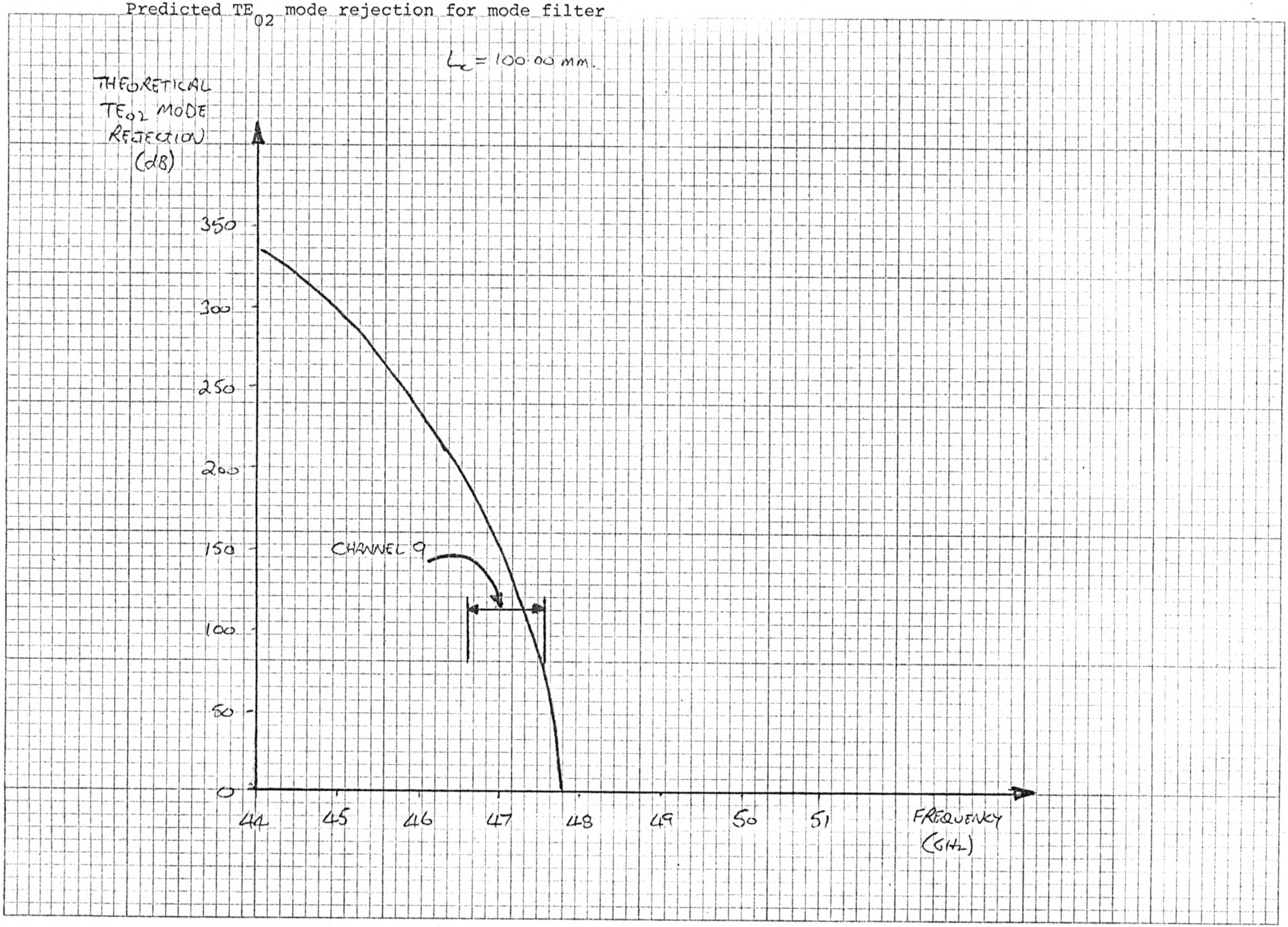

Figure 16
20 mm to 14 mm diameter waveguide taper profile

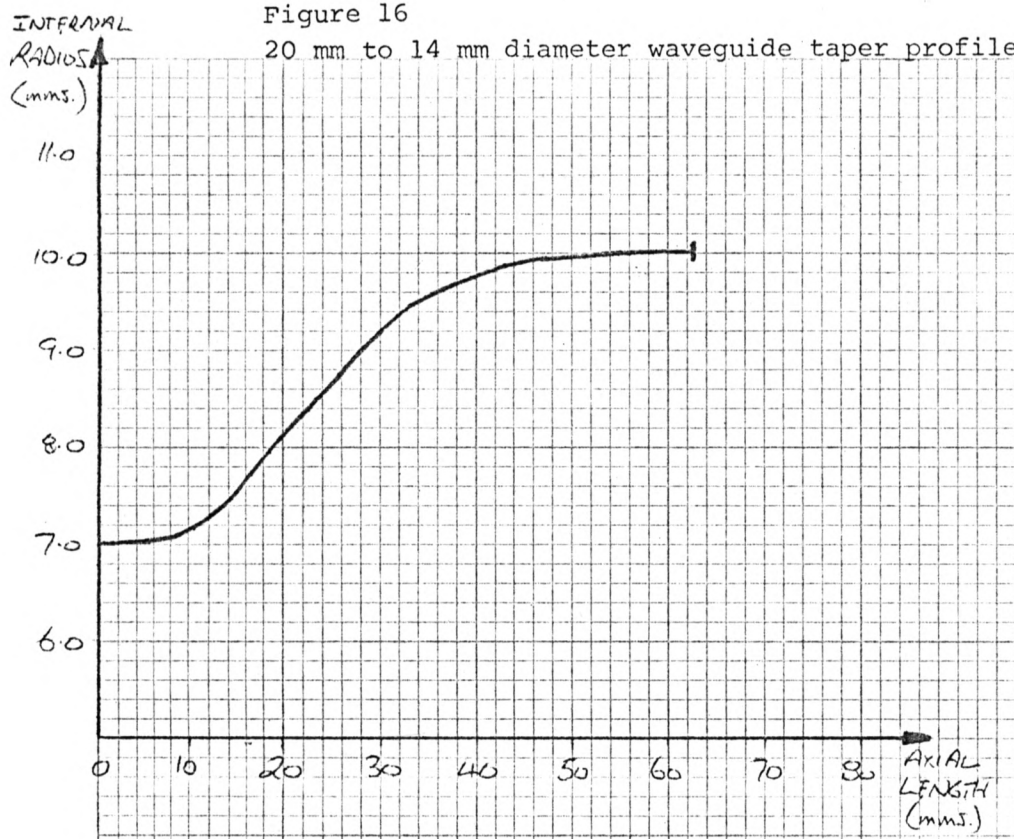

Figure 17

Taper mode coupling near TE_{02} mode cutoff in small diameter waveguide

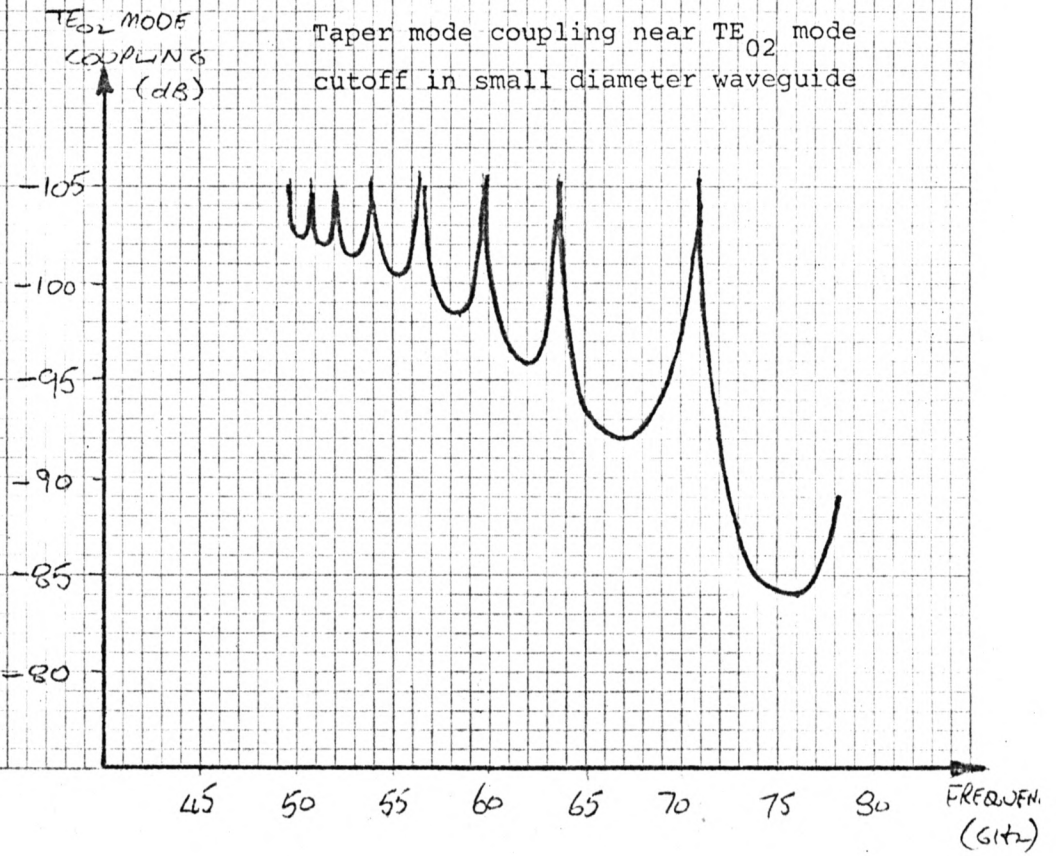

filter is detailed in Appendix B. For a taper mode coupling coefficient of less than -80 dB for frequencies less than 70 GHz, a trial third order sinusoidal coupling distribution, with $\rho(L) = 10.4$, was used. Equations (B1.4) were integrated numerically using this coupling distribution function, resulting in the taper profile shown in Figure 16. This profile has a mode coupling frequency response, predicted by direct integration of the differential equations (B1.1), as shown in Figure 17.

The second requirement implies that the phase response of the filter should not depart from linearity by an appreciable amount over any 50 MHz band of frequencies (the maximum IF bandwidth available in the VLA system) in the TE_{01} mode passband. It is not essential, however, that the overall gradient of the phase response remain constant when measured in different IF bands, since a difference in linear gradient can be compensated by adjusting the delay centers for the relevant antenna IF paths. The worst non-linear phase distortion in this type of filter would be expected to occur at frequencies near the TE_{01} mode cut-off frequency, since the TE_{01} mode phase velocity varies most rapidly with frequency in this region. Figure 18(b) illustrates the phase response of the filter in a 50 MHz bandwidth at the lower frequency edge of channel 1. Figure 18(a) also shows the overall phase response across the full operational TE_{01} mode passband. It can be seen that the deviation from linearity in the lowest frequency 50 MHz band is expected to be less than 1^{o}.

Figure 18 (a)

Phase response of TE$_{01}$ mode filter

On

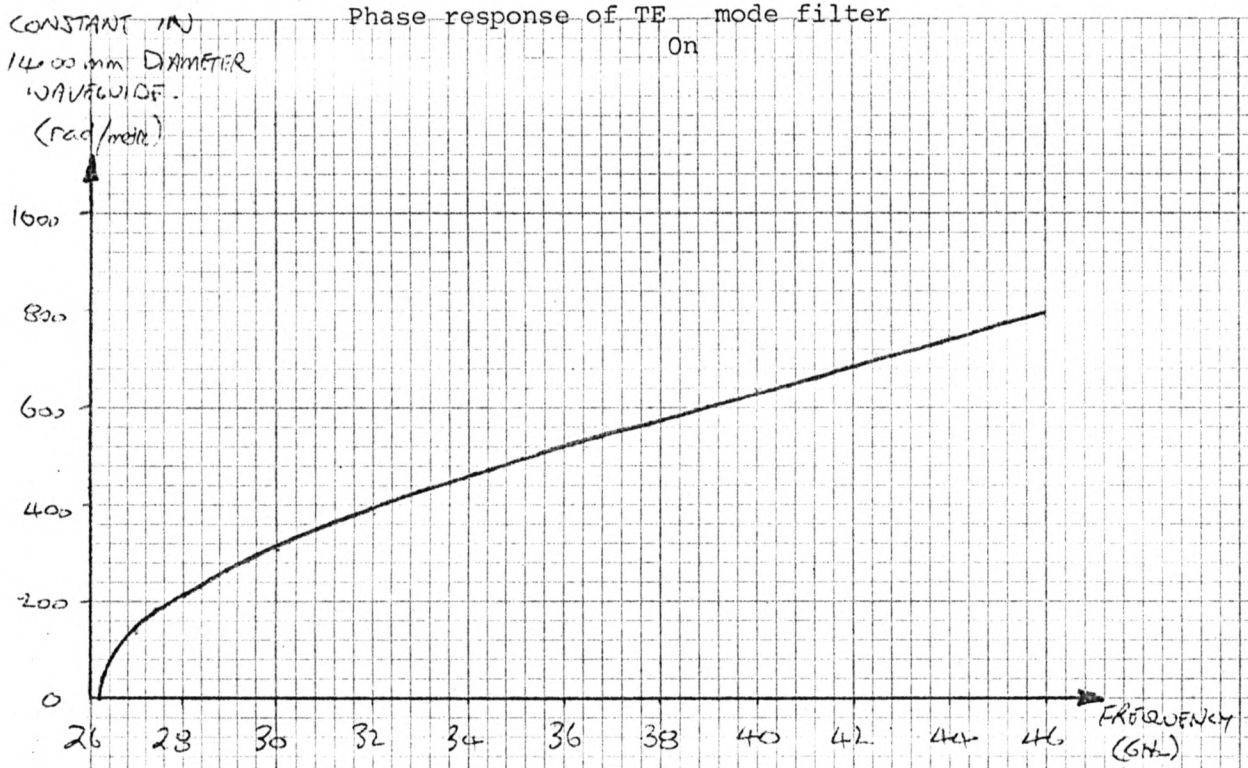

Figure 18 (b)

Phase linearity in lowest IF band

Channel 1

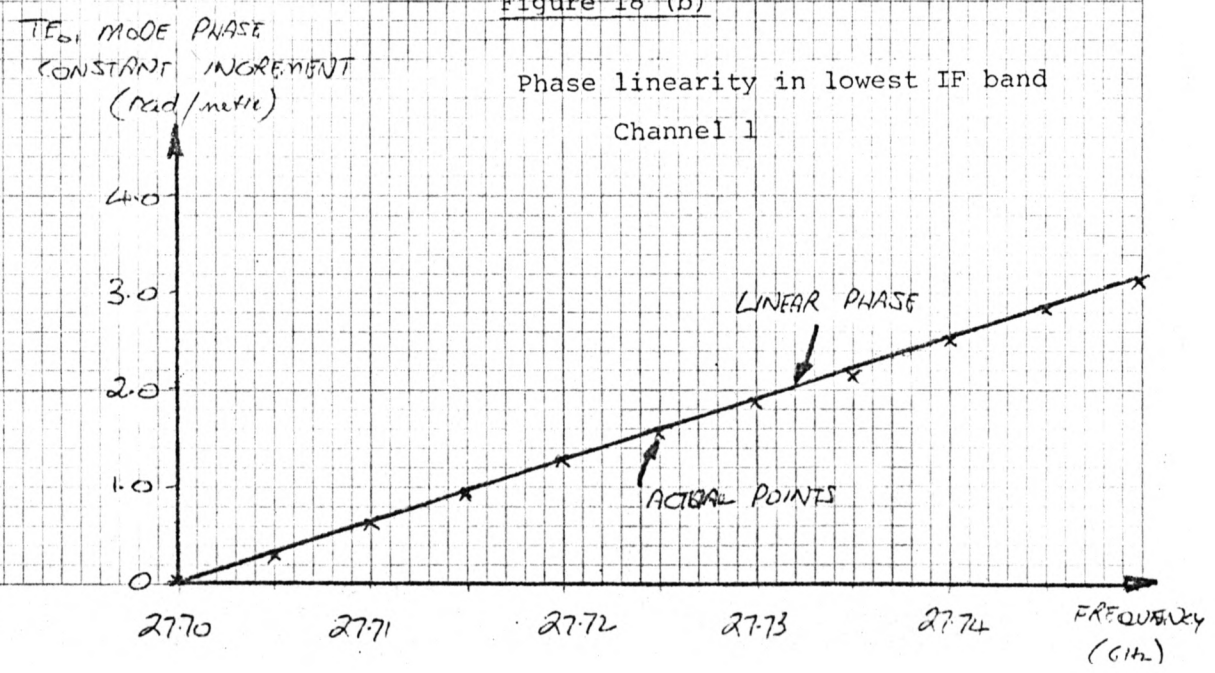

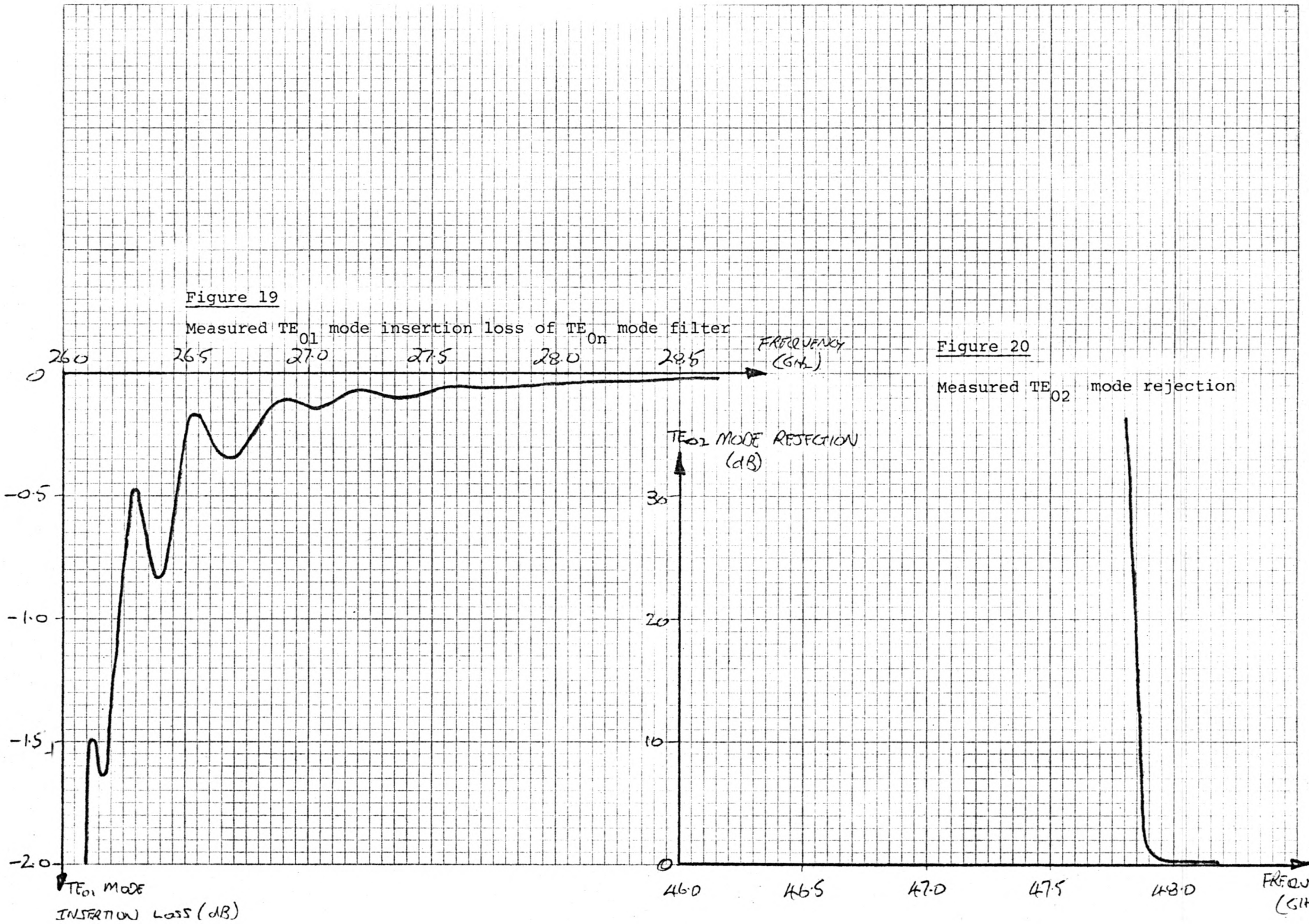

Figure 19

Measured TE_{01} mode insertion loss of TE_{0n} mode filter

Figure 20

Measured TE_{02} mode rejection

The filter has been fabricated by electroforming the device on an accurately machined aluminum mandrel. The taper profile was machined using a computer controlled lathe which used an 8th order polynominal description of the contour. The equal ripple polynominal was fitted to the calculated profile in a least squares fashion to an accuracy of ± 0.006 mm. Standard 20 mm circular waveguide flanges were fitted to the filter after electroforming and machining. The measured TE_{01} mode transmission frequency response is indicated in Figure 19. It can be seen that the insertion loss in waveguide channels 1 through 9 is less than 0.05 dB. The TE_{02} mode rejection and TE_{02} mode generation of the filter have been determined by a similar method to that described in Section 5. The measured TE_{02} mode generation is shown in Figure 20. The TE_{02} mode cut-off frequency was found experimentally to be 47.85 GHz. The TE_{02} mode generation level of the filter was not measurable and is therefore less than -40 dB.

With the mode filter placed in the 20 mm waveguide run from the distribution box to the main trunk waveguide, the station by station mean square variation in the TE_{01} mode transmission response for the southwest arm of the array is as indicated in Figure 21. It can be seen that the expected reduction in ripple at the stations close to the array center is achieved. Furthermore, the small scale frequency dependent variation in the TE_{01} mode transmission response are brought within specification.

Figure 21

Mean square variation in TE_{01} transfer function with mode filter

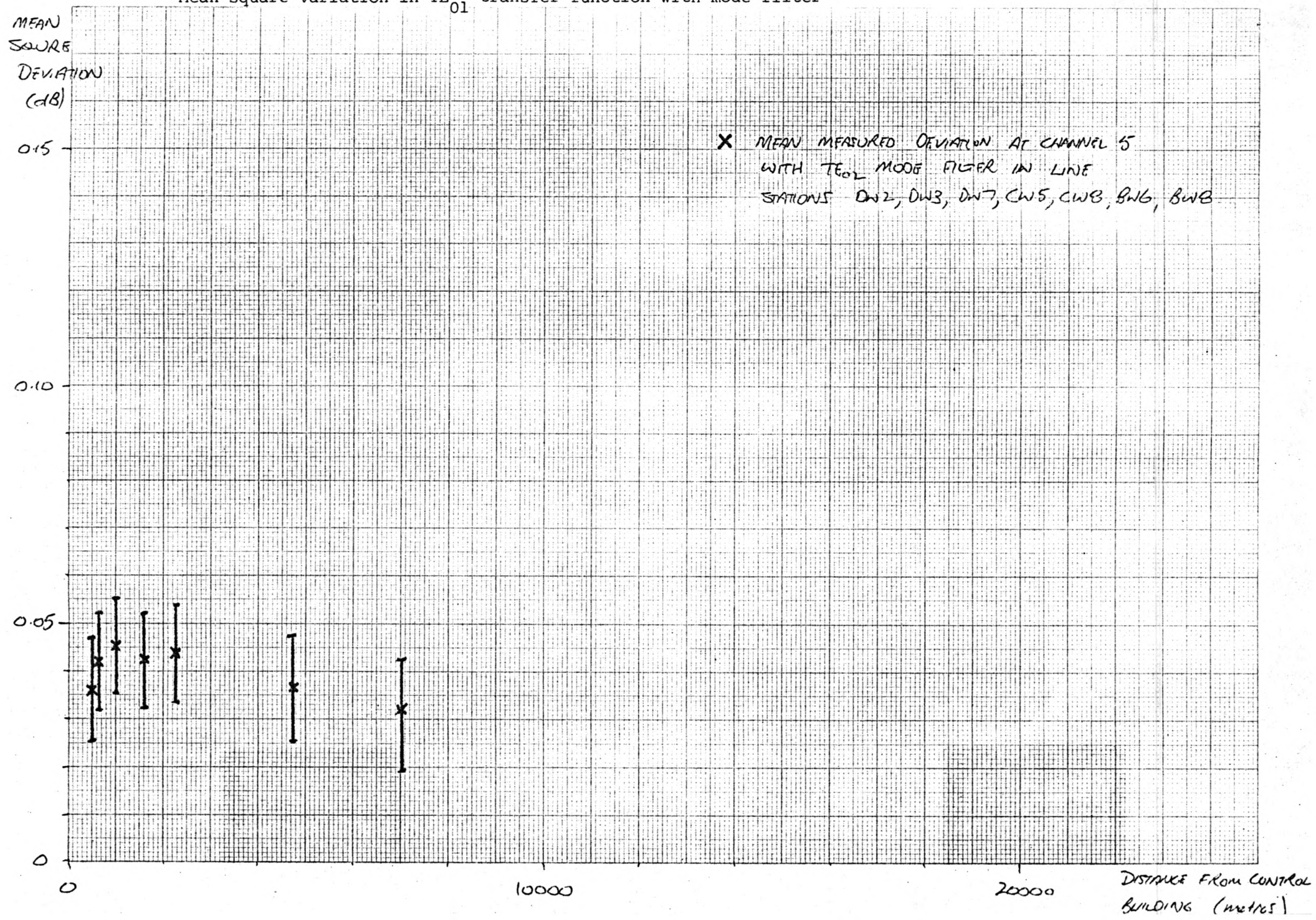

7.0 CONCLUSIONS

Comprehensive analysis and measurement of the TE_{01} mode transmission performance of the VLA waveguide network and its constituent components initially indicated that excessive variation in the TE_{01} response existed at stations within 2.5 km of the center of the array. Furthermore, it was shown that the transmission ripples were due to a higher order mode interaction between the signal distribution box and the coupler coupled arm structure. Fundamental mode reflections or higher order mode interactions between couplers in the main line did not appear to cause significant variation in the TE_{01} mode response. It was shown that, when properly installed, the antenna waveguide system should not result in appreciable degradation of the overall TE_{01} mode transmission uniformity.

A mode filter has been designed and built, which, when installed in the 20 mm waveguide run from the distribution box to the main trunk waveguide line, renders the variation in the overall TE_{01} mode transfer function at any station in the array within specification. The foregoing analysis and measurements have led to the development of accurate broadband techniques for the measurement of TE_{02} mode coupling in overmoded circular waveguide devices. Furthermore, accurate methods for the prediction of circular waveguide taper performance near TE_{02} cutoff have been investigated and a numerical method for the direct integration of the coupling differential operations devised.

APPENDIX A: STANDARD MODE GENERATOR DESIGN EQUATIONS

Referring to Figure 3, let the radius of the smaller waveguide be b and of the larger waveguide, a. Let the transverse electric and magnetic fields of the nth order circular electric mode in waveguide a be $\bar{e}_{an}$, $\bar{h}_{an}$ and in waveguide b, $\bar{e}_{bn}$, $\bar{h}_{bn}$, respectively. Then, following Wexler (1967), the forward and reverse mode coupling coefficients of the dual step transducer are given by the solutions to the following equation sets. Let $\frac{b_1}{a_1}$, and $\frac{b_n}{a_1}$, represent the normalized forward mode coupling coefficients at a waveguide discontinuity and ρ, $\frac{a_2}{a_1}$, and $\frac{a_n}{a_1}$ the reverse mode coupling coefficients, where N modes are considered to exist and interact in the waveguide near the discontinuity plane. Then, the N + 1 boundary reduction equations (A1.1) are first solved for these coefficients for each mode existing in the larger waveguide as incident mode (amplitude a_1).

$$\rho_1 \, I1(n,1) + \sum_{j=1}^{N} \frac{b_j}{a_1} \sum_{i=2}^{N} \frac{I1(j,i)I1(n,i)}{I3(i)} + \frac{b_n}{a_1} I2(n) = I1(n,1)$$

$$\rho \, I3(1) - \sum_{j=1}^{N} \frac{b_j}{a_1} I1(j,1) = -I3(1)$$

$$\frac{a_i}{a_1} = \frac{\sum_{j=1}^{N} \frac{b_j}{a_1} I1(j,i)}{I3(i)} \qquad \text{(A1.1)}$$

where $I1(i,j) = {}_b\int \bar{e}_{bi} \times \bar{h}_{aj} \cdot \bar{i}_z \, ds$

$$I2(i) = {}_b\int \bar{e}_{bi} \times \bar{h}_{bi} \cdot \bar{i}_z \, ds$$

$$I3(i) = {}_a\int \bar{e}_{ai} \times \bar{h}_{ai} \cdot \bar{i}_z \, ds$$

Thus, a set of coefficients $\frac{a_i}{a_k}$, $\frac{b_i}{b_k}$, ρ_k are obtained for all TE_{ok} modes considered incident in the step diameter reduction. These coefficients can be used to derive the reverse scattering parameter of the step at a distance ℓ from the step

$$S_{kj} = \frac{a_j}{a_k} \exp\left\{-(\gamma_j+\gamma_k)\ell\right\} \qquad j \neq k$$

$$= \rho_k \exp(-2\gamma_k \ell) \qquad j = k \qquad \text{(A1.2)}$$

where γ_i is the propagation constant for the ith mode in waveguide a. The N + 1 boundary enlargement equations (A1.3) can then be solved and the transmission and reflection coefficients of the complete mode generator can be derived.

$$\rho I1(1,n) - \sum_{j=1}^{N} \frac{b_j}{a_1} \sum_{i=2}^{N} \left[\frac{I1(i,j) - \sum_{k=1}^{N} S_{jk} I1(k,k)}{I2(i)} \cdot I1(i,n) \right]$$

$$- \left(\frac{b_n}{a_1} + \sum_{j=1}^{N} \frac{b_j}{a_1} s_{jn} \right) I3(n) = -I1(1,n)$$

$$\rho I2(1) + \sum_{j=1}^{N} \frac{b_j}{a_1} \left(I1(i,j) - \sum_{k=1}^{N} S_{jk} I1(1,k) \right) = I2(1)$$

$$\frac{a_i}{a_1} = -\sum_{j=1}^{N} \frac{b_j}{a_1} \frac{\left(I1(i,j) - \sum_{k=1}^{N} S_{jk} I1(i,k) \right)}{I2(i)} . \qquad \text{(A1.3)}$$

For the TE_{on} modes under consideration

$$I1(i,j) = A_a^i A_b^j \frac{2\pi\beta_b^i \omega\mu_o}{h_a^j (k_a^{j2} - k_b^{i2})} J_o(k_b^i b)\, J_1(k_a^j b)$$

$$I2(i) = -A_b^{i\,2} \frac{\pi\beta_b^i \omega\mu_o^{\,2}}{k_b^{i2}} J_o^{\,2}(k_b^i b)$$

$$I3(i) = -A_a^{i\,2} \frac{\pi\beta_a^i \omega\mu_o^{\,2}}{k_a^{i2}} J_o^{\,2}(k_a^i a) \qquad \text{(A1.4)}$$

where A_a^i is a normalization coefficient for the TE_{0i} mode in waveguide a.

β_a^i is the propagation constant for the TE_{0i} mode in waveguide a.

ak_a^i is the ith root of the Bessel function equation $J_o'(ka) = 0$.

APPENDIX B: PREDICTION OF THE PERFORMANCE OF CIRCULAR WAVEGUIDE TAPERS

The coupling between TE_{on} modes in a circular waveguide taper is described by the set of first order differential equations (Tang [1961])

$$\frac{dV_n}{dz} = -j\omega\mu_o I_n + \frac{1}{a}\frac{da}{dz}\sum_{m=1}^{\infty}\frac{2k_m k_n}{k_m^2-k_n^2}V_m \qquad (m\neq n)$$

$$\frac{dI_n}{dz} = \frac{j\beta_m^2}{\omega\mu_o}V_n + \frac{1}{a}\frac{da}{dz}\sum_{m=1}^{\infty}\frac{2k_m k_n}{k_m^2-k_n^2}I_n \qquad \text{(B1.1)}$$

where V_n, I_n are the voltages and current describing the nth mode

$a(z)$ is the waveguide radius at axial position z.

k_i is the ith root of the Bessel function equation $J_o'(k) = 0$.

For a gradual taper, interaction between the TE_{01} and TE_{02} modes predominates, allowing the transformation of the voltages and currents into pairs of forward traveling (A_1, A_2) and reverse traveling (B_1, B_2) waves. Furthermore, if the assumption of a very gradual taper is made, the backward propagation can be neglected, leading to an approximate parametric solution for the taper profile in terms of a function $\rho(z)$, which may be interpreted as an accumulated phase function

$$\rho(z) = \int_o^z \Gamma(z')\,dz'$$

$$\left(\Gamma(z') = \left[\tfrac{1}{4}(\beta_1-\beta_2)^2 + \frac{1}{a^2}\left(\frac{da}{dz}\right)^2\frac{4k_1^2k_2^2}{(k_1^2-k_2^2)^2}\left(\sqrt{\frac{\beta_1}{\beta_2}}+\sqrt{\frac{\beta_1}{\beta_2}}\right)^2\right]^{\frac{1}{2}}\right) \qquad \text{(B1.2)}$$

and a mode conversion distribution function $\Theta(z)$.

The amplitude of the TE_{02} mode wave at the output of the taper of length L is

$$|A_2(\rho_1)| = \left|\int_o^{\rho_1} \Theta e^{2j\rho'} d\rho'\right| \qquad \text{(B1.3)}$$

where $\rho_1 = \rho(L)$

Coupling distributions of the form

$$\Theta = k_n \frac{\ell n(a_2/a_1)}{\rho_1} \sin^n\left(\frac{2\pi\rho}{\rho_1}\right) \qquad \text{(B1.4)}$$

where a_2, a_1 are the final and initial waveguide radii respectively have been used extensively by previous authors (Tang [1961], Unger [1958]) In terms of the distribution function the taper profile is given by the approximate expressions (Hecken & Anuff [1973])

$$a(\rho) = a_1 \exp\left(\int_o^{\rho} \frac{\sin\Theta}{k} d\rho'\right)$$

where $k = \dfrac{2k_1k_2}{k_2^2-k_1^2}$

and $$z(\rho) = \int_o^{\rho} \frac{\cos\Theta}{\Delta\beta} d\rho' \qquad \text{(B1.5)}$$

where $$\Delta\beta(\rho) = \frac{\pi f_o}{c}\left\{\left[1-\left(\frac{k_1 c}{\pi f_o a(\rho)}\right)^2\right]^{\frac{1}{2}} - \left[1-\left(\frac{k_2 c}{\pi f_o a(\rho)}\right)^2\right]^{\frac{1}{2}}\right\}$$

where f_o is the operating frequency and c is the velocity of light in vacuo.

Since backward scattered waves have been neglected, these expressions give a solution which is of inadequate accuracy if the taper is required to give the specified TE_{02} mode coupling distribution when operating near the TE_{02} mode cut-off frequency. In the present application the solution for a(z) given by equations (B1.5) has been substituted into the two mode version of differential equations (B1.1) and the system solved numerically, using the Gear method, for the backward and forward scattered wave amplitudes in order to derive the true coupling distribution at frequencies just above TE_{02} mode cutoff.

The TE_{02} mode relative coupled power level at the output of the taper is given by

$$\rho_{02}(\text{dB}) = 10 \log_{10} \left[\text{Re} \left(\frac{V_2 I_2^*}{V_1 I_1^*} \right) \right] \qquad \text{(B1.6)}$$

APPENDIX C: SPECIFICATION OF THE MAGNITUDE OF THE VARIATION IN TE_{01} TRANSMISSION RESPONSE.

There exist two primary factors which determine the allowable variation in the TE_{01} mode amplitude and phase response of the waveguide communication system. The first is related to the allowable phase deviation between the 5 MHz and 600 MHz local oscillator reference signals at any antenna. The second concerns the desirable peak-to-peak amplitude and phase errors introduced in the IF passbands of a given antenna system as measured at the control building.

The variations may be modeled as a sinusoidal perturbation to the uniform transmission response over a suitable small bandwidth (typically less than 1 GHz). The TE_{01} mode amplitude response as a function of frequency f may be written as:

$$A(f) = A_o + \Delta A \cos (\omega_r f + \phi[L]) \qquad (C1.1)$$

where ω_r is a constant determined by the period of the transmission variations in terms of transmission frequency, ΔA is the peak deviation from a uniform response and $\phi[L]$ is a phase function which depends upon the distance between the discontinuities giving rise to the non-uniform transmission properties.

The TE_{01} mode phase response may similarly be expressed as:

$$\phi(f) = \phi_o f + \Delta\phi \sin (\omega_r f + \phi[L]) \qquad (C1.2)$$

In terms of path delay, τ,

$$T_f = 2\pi\tau = \frac{\phi(f)}{f} \qquad \text{(C1.3)}$$

The phase of the 600 MHz reference signal at any antenna is, assuming a zero reference phase at the central Control Building, given by:

$$\phi^A_{600} = -600\ (T_{1200} + 3\Delta T) \qquad \text{(C1.4)}$$

where $\Delta T = T_{1800} - T_{1200}$, T_f in μs

Similarly, the 5 MHz phase at an antenna is:

$$\phi^A_5 = -5\ (T_{1200} + 241\Delta T^1) \qquad \text{(C1.5)}$$

where $\Delta T^1 = T_{1205} - T_{1200}$

Under normal conditions the LO system is controlled in phase by the 600 MHz reference signal. However, a 5 MHz signal from which the locked signal is derived is continuously compared in phase with the reference 5 MHz. The difference phase is given by:

$$\Delta\phi^A_5 = -5\ (3\Delta T - 241\Delta T^1) \qquad \text{(C1.6)}$$

If this phase difference exceeds ±1 degree, the 600 MHz control is relinquished and the loop lock is transferred to the 5 MHz reference. When 600 MHz relock is again acquired, the 600 MHz loop will have slipped a full cycle in phase, and $\Delta\phi_5$ will have jumped 3^o. This condition is highly undesirable during normal system operation and for this reason $\Delta\phi^A_5$ should be restricted to within the $\pm 1^o$ limits. The 5 MHz phase is most sensitive to variations in the differential delay time ΔT^1, caused by variations in the waveguide ripple structure. The maximum allowable phase ripple must be less

than 1^{o} peak in any 10 MHz band within 200 MHz of the 1200 MHz reference. Then the value of $\Delta\phi_5^A$ will not exceed the limits as the ripple pattern drifts with thermally generated waveguide length changes. The corresponding peak amplitude change is $\pm$0.15 dB. For less than 0.5^{o} peak phase variation, the maximum peak amplitude variation in the TE_{01}, mode transmission response is then $\pm$0.075 dB.

Variations in the TE_{01} mode transmission response can give rise to errors in the measured IF amplitude and phase for a given antenna.

Amplitude variations appear directly as ripples in the IF amplitude response. The analysis of the effect of phase non-linearities is complicated by the application of the 600 MHz round-trip phase correction to the IF phase at the central Control Building. At C-band, the corrected IF phase at baseband (1-2 GHz) with an incident RF signal at the antenna feed of frequency f_o (MHz) and zero reference phase, after transmission through the waveguide system is:

$$\phi_{IF}^{C} = -(f_o - f_{LO1})(T_{f_o - f_{LO1}} - T_{1200}) + (3f_o - 3f_{LO1} - 3600)\Delta Y \quad (C1.7)$$

where f_{LO1} is the first LO frequency (L6) in MHz

$$\Delta Y = T_{1800} - T_{1200}$$

The waveguide has been assumed reciprocal in nature.

This expression may be written:

$$\phi_{IF}^{c} \sim \frac{\Delta\phi_{max}}{2} \left[\frac{(3f_o - 3f_{LO1} - 3600)}{1800} \sin\{1800\omega_o + \phi_1[L]\} \right.$$

$$- \sin\{(f_o - f_{LO1})\,\omega_o + \phi_2[L]\} \qquad \text{(C1.8)}$$

$$\left. - \frac{(2f_o - 2f_{LO1} - 3600)}{1200} \sin\{1200\omega_o + \phi_3[L]\} \right]$$

where $\Delta\phi_{max}$ = peak-to-peak amplitude of waveguide phase ripple across band of interest.

The mean square phase error for changes in the effective length of the waveguide medium may be written approximately as:

$$\overline{\phi_{IF}^{c\,2}} \sim \frac{\Delta\phi_{max}^{2}}{4} \left[1 + 3.086\times10^{-7} (3f_o - 3f_{LO1} - 3600)^2 \right.$$

$$\left. + 6.945\times10^{-7} (2f_o - 2f_{LO1} - 3600)^2 \right] \qquad \text{(C1.9)}$$

For the A channel in C-band, $f_o - f_{LO1} = 1325$ MHz at band center, giving an RMS phase deviation.

$$\phi_{IF\ RMS}^{c} \sim 0.835\Delta\phi_{max} \qquad \text{(C1.10)}$$

If $\Delta\phi_{max}$ corresponds to a 2^{o} peak-to-peak phase ripple in any 10 MHz band in the frequency range 1200-1800 MHz, then the RMS phase error in the IF passband is approximately 1.67. The corresponding decorrelation in any interferometer pair due to waveguide transmission phase ripples of 1^{o} peak amplitude is approximately 0.05%.

It is clear, therefore, that restricting the allowable mean square variation in the amplitude transmission response of the waveguide network to less than 0.05 dB will result in satisfactory performance of the VLA IF/LO system.

REFERENCES

Heeschen, D. S., (1975), Sky & Teles., Vol. 49, pp. 334-351.

Hecken, R. P. and Anuff, A., (1973), IEEE-MTT, Vol. MTT-21, No. 6, pp. 371-380.

Iiguchi, S., (1962), Rev. Ele. Commun. Lab., Vol. 10, pp. 631-642.

Inada K., et al (September, 1973), Fujikura Cabl. Works, Bulletin No. B-2408.

Ogai, M., (1977), NRAO-VLA Elec. Memo. No. 154.

Archer, J., Caloccia, E. and Ogai, M., (1978), NRAO-VLA, Elec. Memo. (in preparation).

Powell, I. L., et al (1977), Proc. IEE, Vol. pp.

Rowe, H. E. and Warters, W. D., (1962), BSTJ, Vol. 41, pp. 1031-1170.

Tang, C. C. H., (1961), IRE-MTT, Vol. MTT-9, pp. 442-452.

Unger, H-G, (1958), BSTJ, Vol. 37, pp. 899-912.

Weinreb, S. et al, (March, 1977), Microwave J., pp. 49-52.

Wexler, A., (1967), IEEE-MTT, Vol. MTT-15, No. 9, pp. 508-517.